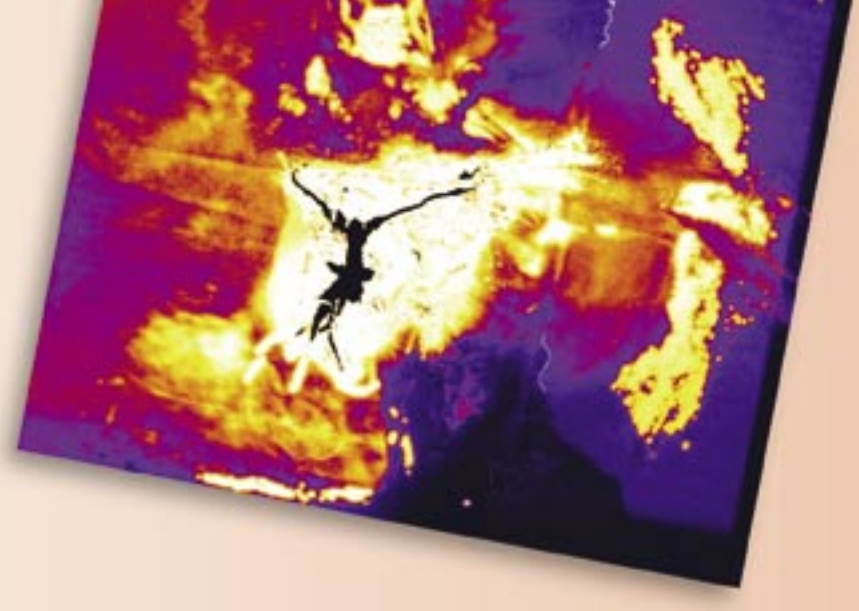

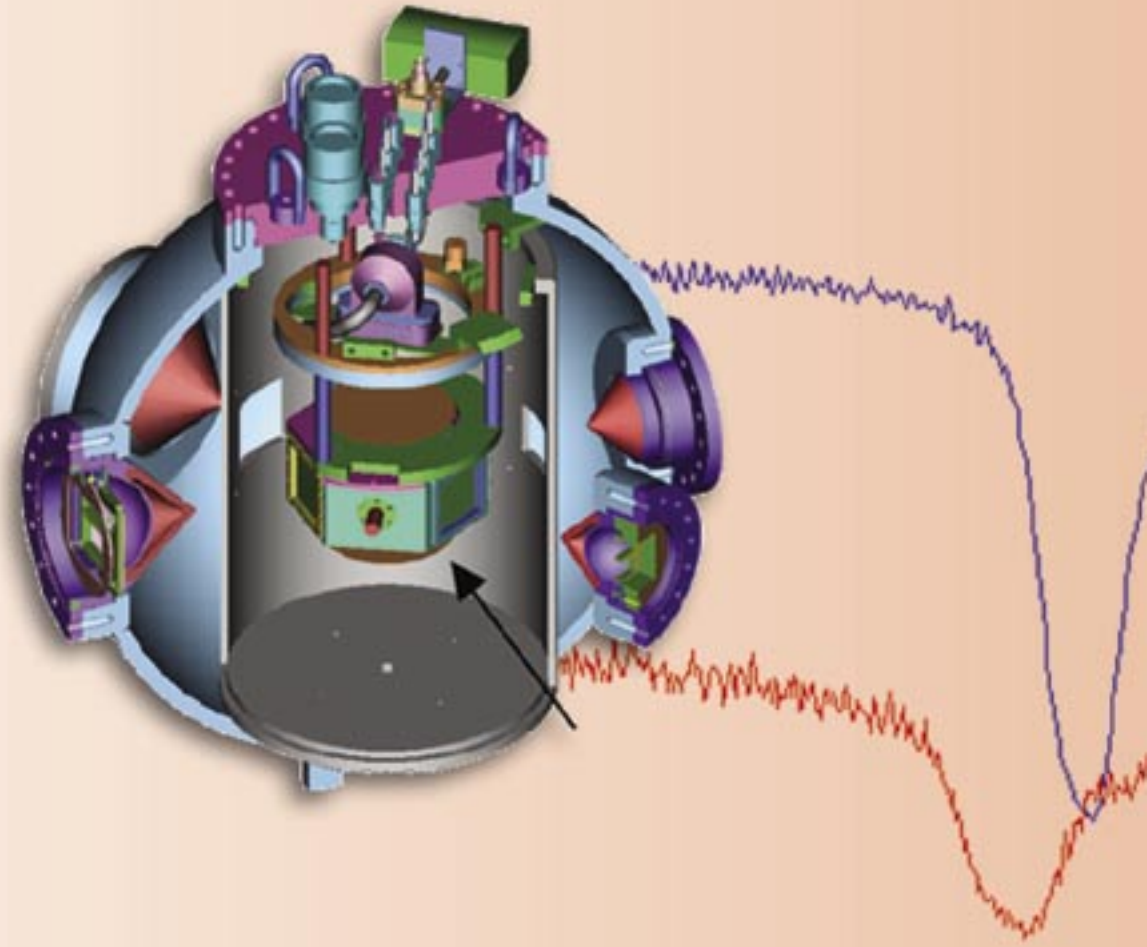

Material Studies

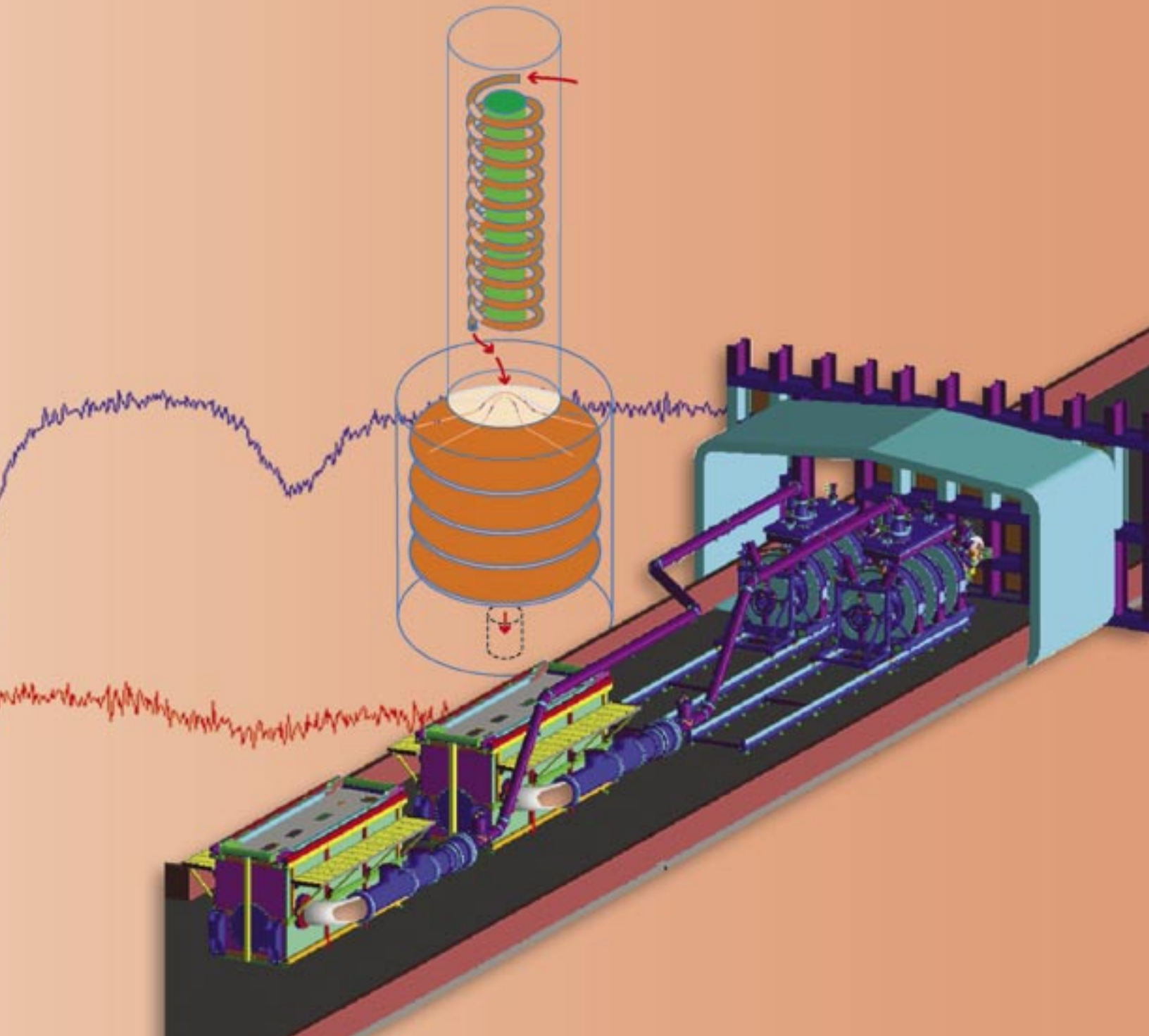

Material Studies Contents

Research Highlights

Dynamic Material Studies in Subcritical Experiments: Rocco, Mario, Vito, and Armando 23
High-Strain-Rate Experiments to Determine the Dynamic Yield Strength of Copper 27
Basic Material Properties Using Laser-Driven Shocks 31
pRad VISAR: An Interferometer-Based Optical Diagnostic for Proton Radiography 35
Temperature of Shocked Materials 39

Project Descriptions

Ejecta Density Measurements Using Soft X-ray Radiography 43
Cross Validation of Ejecta-Areal-Density Measurement Techniques 43
Surface-Temperature Measurements Under Shock Compression 44
Fundamental Properties of Beryllium for ICF Applications 44
High-Speed Pyrometry Measurement of Shocked Tin and Lead 45
Subcritical Experiment Diagnostics 45
SNM Midcourse Detection 46
Sputtering from Fission Fragments 46
Laser-Driven Flyer Plates Generate Shock Waves in Weapons Materials 47
In-Line Holography for Ejecta Particle Size Measurements 47
Equation of State of Beryllium 48
Quantitative Ejecta and Timing Diagnostic Studies 49
Friction Studies at pRad 50
Measurements of the Dynamic Properties of Beryllium Benefit the ICF and Weapons Program 50
Failure-Mechanism Studies of Depleted Uranium Using Proton Radiography 51

Dynamic Material Studies in Subcritical Experiments: Rocco, Mario, Vito, and Armando

R.D. Fulton, M.D. Wilke, N.S.P. King (P-23), representing the Subcritical Experimental teams from Los Alamos National Laboratory, the Atomic Weapons Establishment, Bechtel Nevada, and Sandia National Laboratories

Members of P-22 and P-23 in collaboration with DX, ESA, MST, and X Divisions and with international and national organizations designed and executed a series of SCEs, known as the Stallion series (Vito, Mario, Rocco, and Armando). Mario and Rocco were executed to evaluate the properties (principally strength) of cast and wrought plutonium samples driven by high explosives. Vito was conducted primarily to look at ejecta in a particular region of a weapon. The cast and wrought samples used in our experiments were representative of the materials produced via the different manufacturing processes employed at Rocky Flats and LANL. The specific properties investigated in this series included ejecta production, spall features, and surface temperatures. "Ejecta" is small particulate matter that is "ejected" from the surface of a solid when a strong shock wave interacts with the surface. "Spall" is a general term used for bulk-material failure at the surface of a solid created by a strong shock interacting with the surface. Both ejecta and spall formation depend upon, for example, material strength, grain size, impurities, and other material properties and upon the strength and temporal profile of the shock pressure. An important constraint upon the final state of a shock-driven metal is the surface temperature—which will help further our understanding of the behavior of shocked material.

Vito—Demonstrating a New Technique for the Rapid Turnaround of Subcritical Experiments

Vito, the first SCE in the Stallion series, was fired successfully on February 14, 2002, in the U1a complex at NTS.[1] The experiment—a very successful collaborative effort with LANL, Bechtel Nevada, and the Atomic Weapons Establishment (AWE)(United Kingdom)—achieved a number of important milestones, including the re-establishment of a long-standing LANL-AWE collaboration in performing experiments at the NTS. These historical experiments had been closely aligned with joint theoretical and experimental weapons physics objectives, which are now more focused on maintaining a nuclear-weapons capability without nuclear testing. The second milestone achieved by Vito was a highly successful demonstration of the LANL "racklet" technique (Figure 1). This technique permits the rapid and cost-effective turnaround between SCE experiments with a reuse of diagnostic "clean-room" areas downhole.

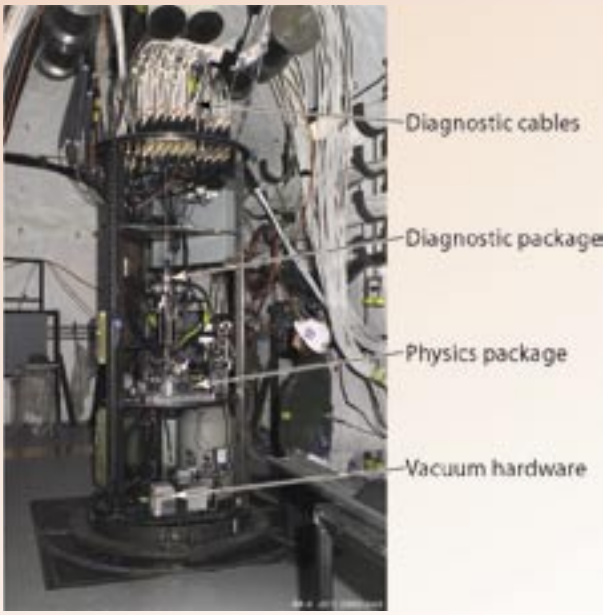

Figure 1. The Vito racklet assembly before it was lowered into the confinement hole.

We obtained a unique data set of high-quality measurements by combining LANL-AWE experimental techniques. Piezoelectric probes[2]

and Asay foils coupled with a laser and streak camera system to record Fabry-Perot and VISAR signatures[3] led to results that enhanced our understanding of the generation of ejecta particles and the distribution of spatially dependent surface velocities. AWE and LANL each provided specialized diagnostics for characterizing the detonation properties of the physics package. Both the physics and the diagnostic packages were shipped separately to the NTS from the AWE and were assembled and installed in the U1a complex. A small team of engineers and diagnostic specialists from AWE were the primary leads for the physics package and the diagnostics measurements. (Improvements to the timing and firing system resulted in an optimized system for future SCEs.) LANL provided electronic readouts for streak cameras that resulted in excellent signal-to-noise ratios in the AWE Fabry-Perot-based velocity measurements. LANL specialists also fielded a VISAR system for data comparison.

In the newly tested racklet technique, both fiber optic and electrical cables enter the experimental chamber from the lid and are routed to the timing and firing system, the energy-release package, the physics package, and the diagnostic package. The diagnostic cables are routed through a secondary containment bulkhead to recording and clean rooms that house digital oscilloscopes, streak cameras, and lasers. We procured special auger equipment to drill a 5-ft-diam, 35-ft-deep confinement hole into the drift invert (tunnel floor). In preparation for the Vito event, the racklet assembly was lowered into a canister that had already been placed into the augered hole to protect the experiment from the surrounding material that would fully confine the experiment. After the Vito event, the cables were cut and moved to a neighboring hole for reuse in another experiment.

Figure 2. Schematic of the diagnostics used on the Mario and Rocco SCEs.

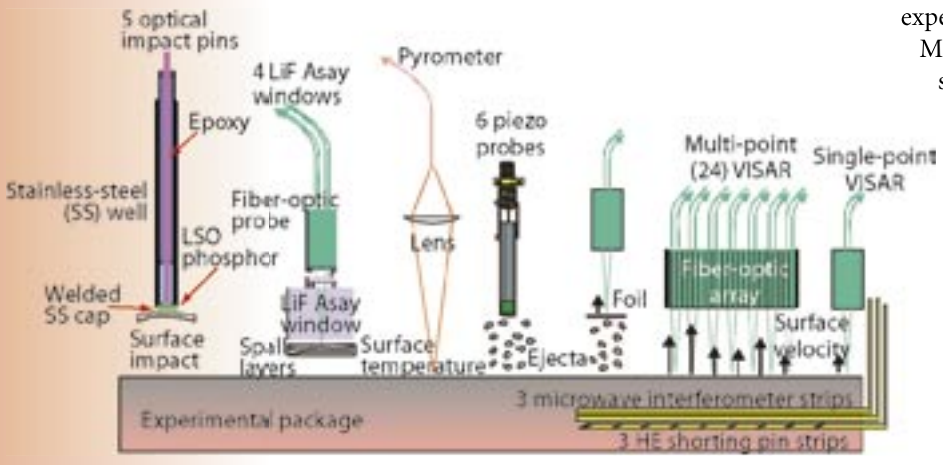

The Vito event demonstrated the success of the racklet technique for SCEs. Through repeated subsequent SCEs, the overall efficiency of the technique was improved, and it now provides a LANL-demonstrated rapid-turnaround capability for the U1a complex. The success of the Vito event resulted in the design of a more complex follow-on collaborative experiment with AWE at the NTS U1a complex.

Mario and Rocco—Addressing the Generation and Dynamic Development of Spall

Mario and Rocco followed the Vito experiment in a collaboration that involved personnel from LANL, SNL, and Bechtel Nevada. The P Division experiments provided important data related to spall, ejecta, and the surface temperature of shocked plutonium in a weapons-relevant geometry. The Rocco and Mario diagnostics and package designs were identical, but Rocco provided data on the physical property of cast plutonium at conditions approaching those found in nuclear weapons to complement the data on wrought plutonium obtained from the Mario experiment.

Like Vito, Mario and Rocco used the racklet technique (described above) for deployment and execution of the physics experiments. But unlike Vito, two "confirmatory" experiments were executed as "dry runs" for Mario and Rocco in 6-ft-diam confinement vessels in the "G" drift region of the U1a complex. Normally conducted at LANL before being executed at the NTS, these confirmatory experiments were conducted at the NTS to better match component delivery schedules, to save time in setting up the diagnostic recording systems, and to eliminate the need to build recording cable plants at both LANL and the NTS. The confirmatory experiments and diagnostics were identical to Mario and Rocco except for the confinement spheres and the use of specially designed surrogate alloys instead of plutonium. Because these surrogate alloys exhibited some of the properties of plutonium, the confirmatory experiments were not only important as dry runs for Mario and Rocco, but they also provided useful data to help interpret the data from Mario and Rocco. The combination of the confirmatory experiments and the actual events were executed with rapidity reminiscent of the heyday of underground nuclear testing.

The Mario and Rocco experiments addressed material-physics issues (in particular, the generation and dynamic development of spall) that were used in computer simulation codes to model the nuclear-explosion process. The high-quality data obtained from Mario and Rocco were important both for their significance to the SCE program and for execution of the upcoming Armando SCE (described below), which will image identical experimental packages via x-ray radiography to measure the spatial distribution of the spall layers. Rocco used the same diagnostic suite as Mario to make a direct comparison between the behavior of wrought and cast plutonium under shock conditions.

The diagnostics used in the Mario and Rocco shots (Figure 2) included line VISAR, point VISAR Asay foil (which measures ejecta mass), Asay windows, piezoelectric probes, optical pins, and infrared pyrometry. Electrical pins and flat Mylar microwave-interferometry strips inside the high explosive measured its performance. P Division and SNL developed the Asay-window diagnostic for the Mario and Rocco experiments. Information on the state and thickness of the spalled layers below the target surface can be inferred by allowing these layers to collide in a "domino fashion" into an LiF window and by observing the change in velocity of the metal-LiF interface. A number of small high-explosive-driven experiments were conducted in firing chambers at DX and at the LANL pRad facility to validate individual diagnostic techniques, particularly the Asay window technique, with modeling support from X Division.

Armando—Verifying Surface Behavior Observed on Mario and Rocco

Armando—the last of the SCEs in the Stallion series to be executed in April 2004—will use a reduced set of the diagnostics deployed on Rocco and Mario, including point VISAR, surface velocity diagnostics, and optical pyrometers, to verify the behavior of the target surface observed in the Rocco and Mario shots. The primary diagnostic for Armando will be x-ray radiography along two equivalent axes separated by 60°. Physics packages identical to those used in the Rocco and Mario shots will be combined in a hexagonal (HEX) package (six sides) vertically separated with the free surfaces facing one another. This geometry will allow us to obtain equivalent x-ray radiographs of the two materials at the same time in their dynamic evolution. The third axis of the HEX package will be used for VISAR and pyrometry access.

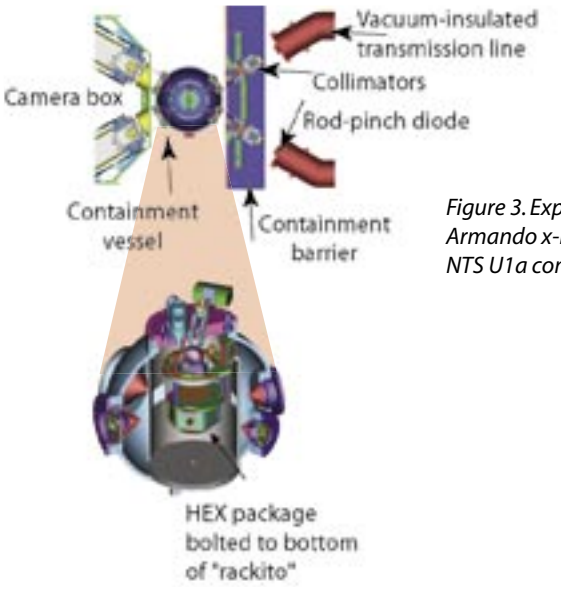

Figure 3. Experimental layout of the Armando x-ray radiographic system at the NTS U1a complex.

The experimental package will be in a 3-ft-diam (inside diameter) confinement vessel. This vessel and a camera box that houses an x-ray-to-light-converting scintillator and camera system will be placed within a "zero room" created by a large bulkhead. (The term "zero room" is derived from "ground zero"—the location on the surface beneath which a nuclear event was detonated in the days of underground testing. The SCE is contained within the zero room.) Thin radiographic windows in the bulkhead and confinement vessel allow x-rays to pass through the package and the confinement vessel with minimal attenuation (Figure 3). By fielding the experiment within a confinement vessel, the zero room can be reused for multiple experiments.

The Cygnus x-ray sources (Figure 4) will extend down a drift external to the zero room. These sources will be composed of a Marx bank system, which will be contained in a large oil-filled tank that will pulse-charge an adjacent pulse-forming line (PFL). The output of the PFL will be a short (60 ns), large-amplitude (1 MV) electrical pulse that will propagate down an 8-in.-diam, water-filled, coaxial transmission line. This electrical pulse will be coupled into inductive voltage adder cells that will add the voltage in parallel to produce a 2.25-MV low-impedance drive pulse for the rod-pinch diode. This last stage of voltage addition will be accomplished in a high vacuum suitable for diode operation.

The radiography that will be used on the Armando SCE represents a significant leap in performance. It

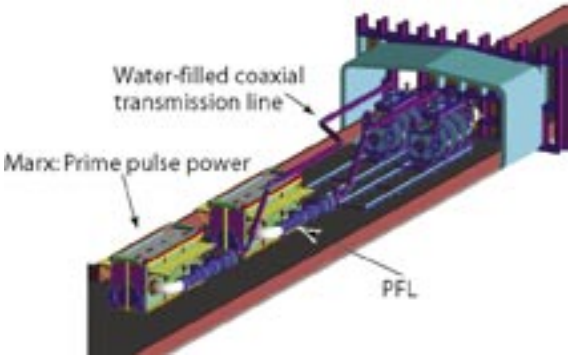

Figure 4. Layout of Cygnus x-ray sources in the U1a.05 drift (tunnel) at the U1a complex.

has been the result of a multi-year, multi-laboratory effort involving LANL, SNL, AWE, Bechtel Nevada, the Naval Research Laboratory (NRL), the Titan Corporation Pulse Sciences Division, and the Mission Research Corporation. Many innovations have combined to lead to this leap in performance, but perhaps the most important has been the effective realization of the rod-pinch diode originally developed at NRL. The rod-pinch has a similar geometry to standard x-ray diodes that have been used in industrial flash x-ray sources for several decades. However, NRL discovered that, when operated at low impedance (large currents at ~ 40 kA), the diode would transition from classic space-charge-limited flow into magnetically limited flow, whereby the electrons would be transported to the end of the central anode rod and then "pinch," thus producing a very bright, small diameter x-ray source. The Cygnus x-ray source was designed to provide a low-impedance source of voltage to effectively drive the diode into the magnetically limited regime. Measurements have demonstrated a 1-mm-diam x-ray spot that produces 4 rad at 1 m in a reproducible manner.

The detector system is equally innovative. It combines technologies developed for DARHT and pRad to create a very high-resolution imaging system. The detector converts the x-rays transmitted through the experimental package into visible light in a tiled, cerium-doped LSO (lutetium oxyorthosilicate) scintillator, which makes the high efficiency and high resolution of the detector system possible. The light produced is transported by a lens system to an LN_2-cooled charge-coupled-device (CCD) chip that captures and records the image. To preserve maximum image resolution, the combined CCD camera system is not gated; all time resolution therefore derives from the flash nature of the illuminating x-ray pulse. The scintillator-camera combination must, however, be maintained in a light-tight configuration throughout the high-explosive detonation and long enough thereafter (~ 30 s) for the information to be read out of the CCD camera system to a remote data-logging computer.

Conclusion

To date, the Stallion SCE series has provided high-quality information of critical importance to the LANL design effort while simultaneously helping to reinvigorate the mutually beneficial collaboration with AWE on weapons-physics experiments. Execution of the final experiment in the series—Armando—will provide high-quality radiographic data previously unobtainable and will result in a facility that is ideally suited to further investigate the dynamic properties of plutonium under shock loading.

References

1. N.S.P. King, "The Vito/Etna subcritical U1A experiment," *Weapons Insider* **9(1),** 1–2 (2002).
2. C.S. Speight, L. Harper, and V.S. Smeeton, "Piezoelectric probe for the detection of shock-induced spray and spall," *Review of Scientific Instruments* **60(12),** 3802–3808 (1989).
3. J. Asay and M. Shahinpoor (Eds.), *High-pressure shock compression of solids* (Springer-Verlag, New York, 1993).

Acknowledgment

These types of experiments could not have been performed without the efforts of a large number of colleagues from DX, P, ESA, MST, and X Divisions at LANL and from SNL, Bechtel Nevada, and the AWE. This work was sponsored by DOE Defense Programs.

For more information, contact Robert Fulton at 505-667-2652, fulton_robert_d@lanl.gov.

High-Strain-Rate Experiments to Determine the Dynamic Yield Strength of Copper

R.T. Olson, D.T. Westley, B.G. Anderson, L.J. Tabaka, J.S. Ladish, J.L. Stokes (P-22), W.L. Atchison (X-1), G. Rodriguez, Q. McCulloch (MST-10). J.H. Goforth, H. Oona (DX-2), R.E. Reinovsky (P-DO), representing colleagues from the All-Russian Scientific Research Institute of Experimental Physics, Sarov, Russia

A series of experiments, known as the Russian High Strain Rate (RHSR) experiments, has been designed and partially completed to determine the dynamic yield strength of copper. The data obtained from this experimental series are used to validate theoretical and computational models of material behavior at high strains (100%–150%) and strain rates (~ 10^6 /s).[1] To achieve these high strains and strain rates, a two-stage explosively driven pulsed-power generator is used to produce high currents that magnetically implode a cylindrical aluminum liner onto a copper sample. The sample, also cylindrical, incorporates machined sinusoidal perturbations of two different wavelengths on its outer surface. Theoretical models predict that the growth rate of these perturbations is wavelength dependent and directly related to the dynamic yield strength of the copper.

The RHSR experiments are important to refine and validate computational models of dynamic material strength under high-strain and strain-rate conditions. Validation of such models is an essential element of the ASCI-code-development effort that will support nuclear-weapons certification in the future. Additionally, these experiments have the added benefit of fulfilling a goal of the National Nuclear Security Administration (NNSA) to significantly increase collaboration between Russian and U.S. weapons laboratories on fundamental science issues.

Experimental Design

Because the Atlas pulsed-power capacitor bank is presently being relocated from LANL to the NTS, the high currents needed to perform this type of experiment are currently not easily attainable in the U.S.[2] However, the VNIIEF scientific research institute in Sarov, Russia, has developed an explosively driven pulsed-power generator that can supply the required 35-MA current.[3] The VNIIEF device consists of two parts: a helical explosive magnetic generator (HEMG) and a multi-element disk explosive magnetic generator (DEMG) (Figure 1). Both devices use rapid magnetic flux compression to generate a very high, short pulse of electrical current. The basic concept behind these devices is that a small "seed" current creates magnetic flux through a volume within the generator. Igniting high explosives rapidly collapses this volume, and because the flux is initially preserved, a portion of the work done by the high explosive is converted to electrical current. In the case of the RHSR device, the HEMG delivers 6.5 MA as the "seed" current for the DEMG that in turn delivers ~ 35 MA through a liner inside the physics package.

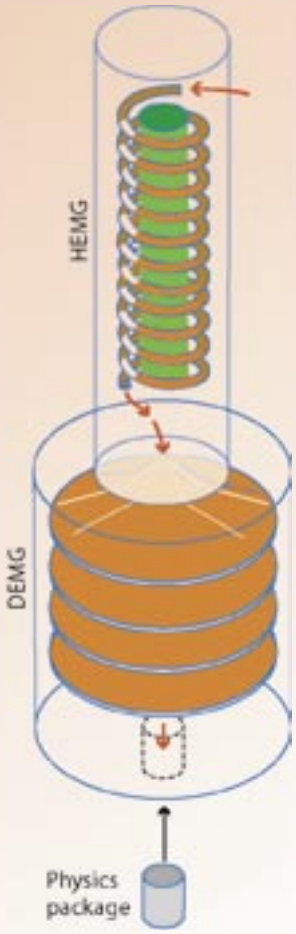

Figure 1. The combination of the HEMG and DEMG deliver a peak current of ~ 35 MA through the liner in the physics package.

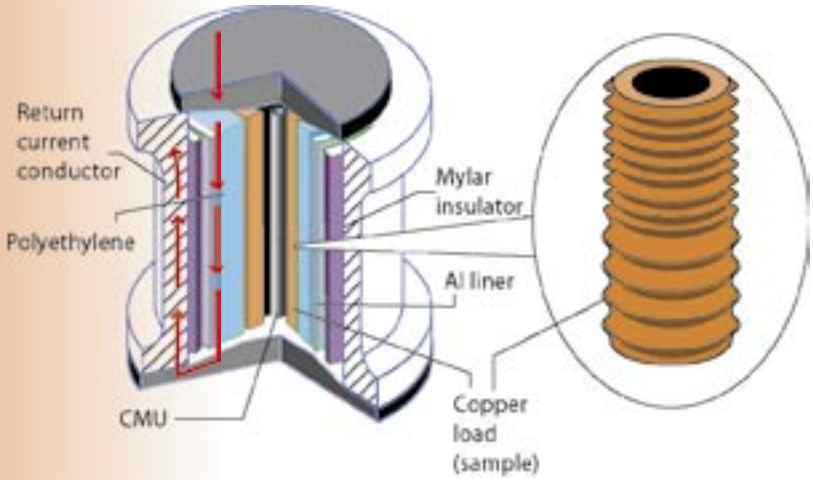

Figure 2. The cylindrically symmetric physics package contains a copper sample that is imploded by the aluminum liner.

The liner is an aluminum cylinder with a 4-mm-thick wall and an inner diameter of 96 mm. The current flowing through it causes the liner to magnetically implode and push on polyethylene that fills the entire space between the liner and a 52.6-mm-diam copper sample (Figure 2). The copper sample has 2.0- and 4.0-mm-wavelength sinusoidal perturbations machined on its exterior surface with initial amplitudes of 1.0 mm. The volume inside the cylindrical copper sample is evacuated and contains a stainless-steel central measuring unit (CMU).

During the implosion, the polyethylene shocklessly transfers the pressure from the liner to the copper cylinder causing it to radially compress to a peak pressure of 160 kbar at a strain rate of ~ 9 x 10^5/s. Under these conditions, the copper-polyethylene interface is Rayleigh-Taylor unstable, and the perturbations will grow as a function of time during the implosion.[4,5] The design of the RHSR experiments assumes that the dynamic yield strength of polyethylene is small enough that it can be neglected, and as a result, its hydrodynamic properties closely approximate those of a fluid. This assumption is important because it allows the dynamic yield strength of the copper to be determined directly from the growth rate of the perturbation amplitude.

Experimental Diagnostics and Data

A Faraday rotation diagnostic is used to measure current delivered from the DEMG to the load as a function of time.[6] The diagnostic consists of a single-mode quartz fiber that encircles the entire electrical current path to the liner. An 830-nm laser diode injects linearly polarized light into the fiber, and current flowing through the load creates a magnetic field that causes the polarization of the light in the fiber to rotate. The light rotation angle is subsequently detected using an optical polarization analyzer once it exits the fiber. The time-dependent current through the load is then calculated using the Verdet constant (2.65 +/- 0.03 rad/MA) of the fiber that relates the light-polarization rotation angle to the enclosed current. Because this measurement technique is only sensitive to current that passes through the area defined by the fiber loop, an accurate measure of the current through the liner can be obtained.

A B-dot is an inductive probe that consists of a center-wound wire loop inserted into current-carrying regions of the load, HEMG, and DEMG. Current flowing in the region of the B-dots generates a time-varying magnetic field that induces a small current in each B-dot loop. This B-dot signal is proportional to the time derivative of the current flowing in the experimental device. Because the B-dot is extremely sensitive to changes in current, it provides critical timing information about the performance of the device, including the start of current flow, peak current time, and copper impact on the CMU.

Thus far, two of the three planned experiments have been performed: RHSR-0 and RHSR-1. The peak current, as measured with the Faraday rotation diagnostic, was 34.9 MA for RHSR-0 and 34.6 MA for RHSR-1 (Figure 3). The B-dot data obtained from the RHSR-0 experiment shows that peak current occurred at 27.1 μs after the high-explosive detonator in the DEMG was initiated.

A VISAR is an interferometer used to measure the velocity of a reflective surface as a function of time.[7,8] The VISAR uses a 532-nm laser coupled to a glass fiber that transports the light to the inside surface of the copper load via the CMU. Light reflected from the copper surface is recollected and transmitted down a separate glass fiber to an interferometer. Upon entering the interferometer, the reflected light is split into two optical paths with different optical lengths and subsequently recombined to interfere with one another. Motion of the copper sample produces a Doppler shift in the recollected light and, as a result, an interference fringe shift that is recorded as a function of time. The velocity of the reflective copper surface is proportional to this fringe shift and was measured to be 3.1 mm/μs at impact with the CMU in both

RHSR-0 and RHSR-1. Additionally, the VISAR data indicated the impacts occurred 32.5 μs after the DEMG detonators were initiated (Figure 4). These data provide information about both the load hydrodynamics as a function of time and the time when the load reaches a radius of 10 mm during the implosion.

Low-energy x-ray radiographs were obtained to measure the perturbation growth of the load at three distinct times during the hydrodynamic explosion. Two different x-ray source designs were used in the experiments: one was designed and built by LANL, and the VNIIEF team provided the other. The LANL x-ray source consists of an x-ray head coupled to a 900-kV Marx bank via ~ 20 m of coaxial cable.[9] The x-ray head contains a 1.5-mm-diameter tungsten anode, which generates a 20-ns-long x-ray pulse. The x-ray spectrum of this pulse is comprised primarily of K_α-line and Bremsstrahlung radiation with an endpoint energy of ~ 350 kV.

Transverse x-ray radiographs of the dynamically evolving copper perturbations are acquired by locating the x-ray heads and films on opposite sides of the load. A steel enclosure protects the film from shrapnel generated by the ~ 175-lb high-explosive charge in the DEMG and the aluminum-return-current conductor. The film is recovered after the experiment to be developed and digitized for later analysis.

The flash x-ray sources were fired to record images from ~ 1.5 μs before impact to ~ 1.5 μs after impact of the copper sample upon the CMU. These radiographic times were chosen to provide images both during the shockless perturbation growth phase of the implosion and to observe the effect of the reflected shock generated upon impact with the CMU. Only the single radiograph produced with the VNIIEF x-ray source was successfully recovered from RHSR-0. Damage to the LANL films by the high explosive and shrapnel prohibited any additional successful data retrieval. Improvements in the film protection systems enabled the successful recovery of all three radiographs from the RHSR-1 experiment, although each piece of film sustained moderate to severe shrapnel damage.

The radiographs from both experiments showed shockless-perturbation-amplitude growth of $A/A_0 \sim 2$–3 before CMU impact. The amplitude then rapidly dropped to $A/A_0 \sim 0.7$ once the reflected shock exited the copper sample (Figure 5). Given the assumption that the polyethylene moves and flows like a fluid under these dynamic conditions, the perturbation amplitude exhibited significantly less growth than the $A/A_0 \sim 8$–12 predicted by the theoretical models. There are two possible explanations for this result: (1) the strength model used in the computations does not adequately describe the dynamic strength properties of copper, or (2) the assumption that the polyethylene was a dynamically strengthless material is invalid.

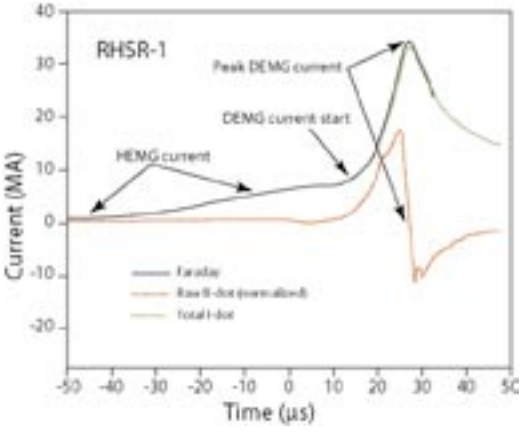

Figure 3. B-dots, proportional to the time derivative of current flowing in the DEMG, indicate peak current occurred at 27.1 μs after detonator initiation. The Faraday rotation diagnostic recorded a peak current of ~ 35 MA.

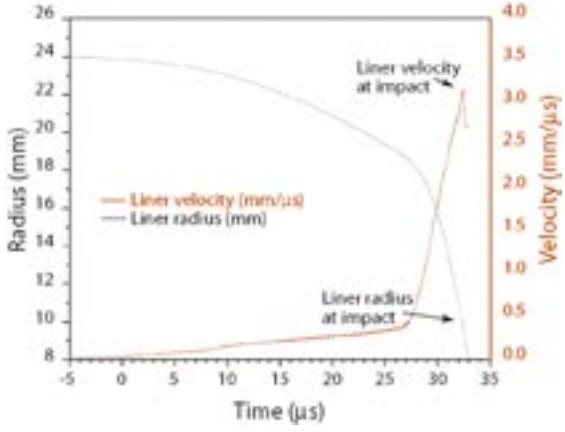

Figure 4. VISAR data indicates the inner surface of the copper is moving 3.1 mm/μs at impact with the CMU.

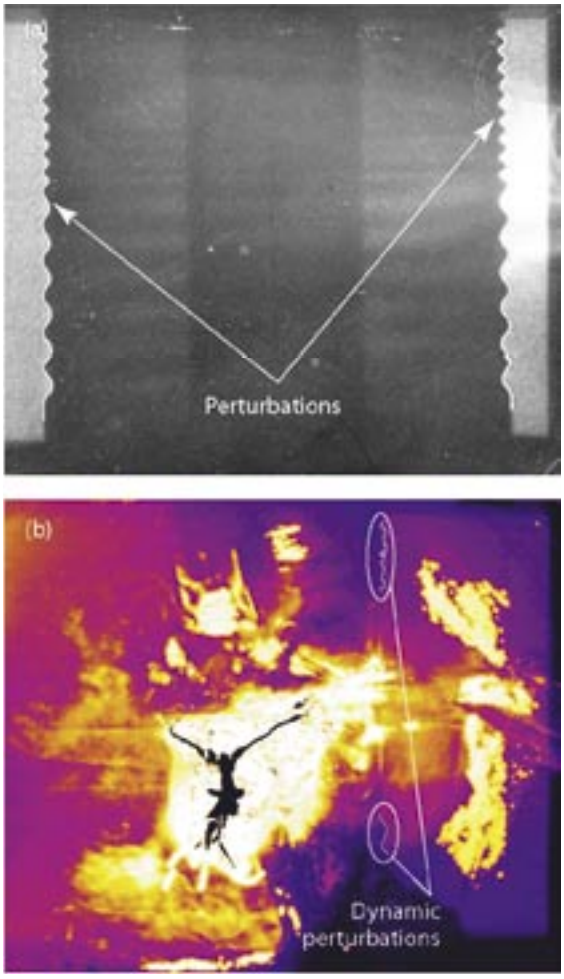

Figure 5. The static (a) and dynamic (b) x-ray radiographs acquired by LANL show the RHSR-1 perturbation edges with the dynamic image quality significantly affected by shrapnel damage. The dynamic radiograph was acquired 1.0 µs after impact of the copper on the CMU.

Conclusion

RHSR-2 is currently being designed using a liquid material (such as butane, water, or ethylene glycol) to eliminate the ambiguity introduced by the polyethylene. However, given this change in materials, a redesign of the load is necessary to maintain the same shockless condition in the fluid that was present using polyethylene in the RHSR-0 and RHSR-1 experiments. The RHSR-2 experiment with its redesigned load is currently scheduled for February 2004.

References

1. D.J. Steinberg, S.G. Cochran, and M.W. Guinan, "A constitutive model for metals applicable at high-strain rate," *Journal of Applied Physics* **51**, 1498 (1980).
2. R.E. Reinovsky *et al.*, in *Proceedings of the 2003 IEEE International Pulsed Power Conference* (Dallas, TX), in publication (2003).
3. V.K. Chernyshev *et al.*, in *Proceedings of the 1997 IEEE International Pulsed Power Conference* (Baltimore, MD), pp. 1441–1447 (1997).
4. D.H. Sharp, "An overview of Rayleigh-Taylor instability," *Physica D* **12**, 3 (1984).
5. M.G. Sheppard *et al.*, in *Proceedings of the 1997 IEEE International Pulsed Power Conference* (Baltimore, MD), pp. 1399–1403 (1997).
6. J.L. Stokes *et al.*, in *Proceedings of the 2001 IEEE International Pulsed Power Conference* (Las Vegas, NV), pp. 365–367 (2001).
7. L.M. Barker and R.E. Hollenbach, "Laser interferometer for measuring high velocities of any reflecting surface," *Journal of Applied Physics* **43**, 4669 (1972).
8. W.F. Hemsing, "Velocity sensing interferometer (VISAR) modification," *Review of Scientific Instruments* **50**, 73 (1979).
9. B.G. Anderson *et al.*, in *Proceedings of the Ninth International Conference on Megagauss Magnetic Field Generation and Related Topics*, (Moscow, Russia) in publication (2003).

Acknowledgment

The authors would like to acknowledge the efforts of the numerous individuals both at LANL and VNIIEF who provided the essential logistical support necessary to conduct these experiments. Without these people acting as interpreters, manufacturing parts, arranging travel, and shipping equipment through customs, the RHSR experimental series would not have happened. This work is supported by the NNSA via the Office of Defense Programs.

For more information, contact Russell Olson, 505-667-6667, rtolson@lanl.gov.

Basic Material Properties Using Laser-Driven Shocks

D.C. Swift, A. Hauer, D. Paisley, J. Niemczura, T. Tierney, R. Johnson (P-24), J. Wark, A. Loveridge, A. Allen (University of Oxford), B. Remington, D. Kalantar (LLNL), D. Thoma, J. Cooley, R. Hackenberg (MST-6), K. McClellan (MST-8), A. Koskelo, S. Greenfield (C-ADI), P. Peralta, E. Loomis (Arizona State University)

Shock waves can be induced in samples by illumination with an intense laser; pressure is generated as the target absorbs energy, and atoms are ablated from the surface to form a plasma plume. Our team is investigating the response of materials to dynamic loading using the Trident laser with *in situ* optical and x-ray diagnostics complemented by post-shot microstructural analysis.

Accurate models of the response of materials to dynamic loading are important for simulations of the performance and safety of weapons and for the design of the fuel capsule in ICF. These models are devised and calibrated using experiments in which samples are subjected to high pressures, usually from shock waves induced by the detonation of high explosives or the impact of flyers.[1] New classes of models are being developed that use more detailed underlying physics, such as dislocation dynamics, rather than *ad hoc* empirical relations to describe the response. Laser-driven materials experiments offer promising possibilities to contribute to model development, including convenient new diagnostics such as transient x-ray diffraction (TXD) to measure the response of materials at the microstructural level.

Laser-Induced Shock Experiments

Shock waves—whether induced by laser ablation or more traditional methods—can be regarded as a region of high pressure that moves through a body of material. By measuring the response as material is subjected to dynamic loading and unloading, we can understand its behavior in terms of a pressure-volume-temperature relation (often called the EOS), phase diagram, phase-change kinetics (including chemical reactions), plasticity, and fracture. The simplest measurement is the speed of the shock wave, from its transit time through the sample. The velocity imparted to the material by the shock is inferred from the velocity history at the surface of the sample; features in the velocity history also provide information about plasticity and phase changes.[1] We have developed and applied other diagnostics on laser experiments. TXD—applied to single crystals and polycrystalline ensembles—provides detailed information on the shock response of material at the level of the atomic lattice, including plasticity and phase changes.[2,3] Ellipsometry measures the polarization-dependent reflectivity of a surface and can be a sensitive test for phase transitions. We have recorded surface velocity and displacement in one and two spatial dimensions—with time resolution as well—to investigate the effect of a material's microstructure on shock propagation.[4,5]

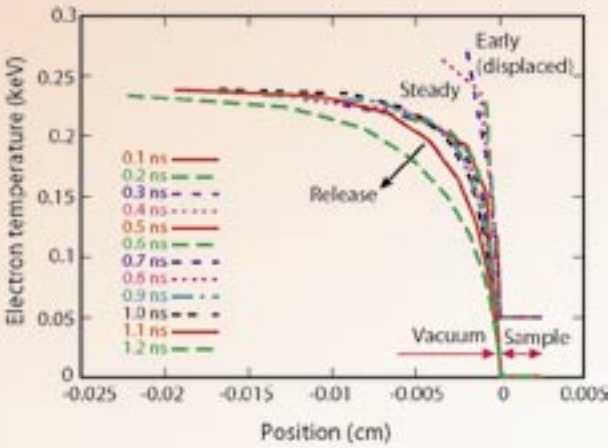

Figure 1. Profiles of electron temperature at different times during the interaction of a 1-ns-long laser pulse and 1 PW/m² with a 25-μm-thick iron target .

Laser-induced shock experiments have some disadvantages compared with traditional shock techniques. Principally, it is more difficult to ensure that the shock has a constant pressure. (Conversely, it can be easier to induce other loading histories such as multiple shocks, decaying shocks, and isentropic ramp waves.) However, using a laser to induce the initial shock wave can make it easier to apply new diagnostics, because synchronization is generally more straightforward than with shocks launched by explosives or a flyer impact. Also, compared with other techniques, it is often easier to recover shocked samples from laser experiments.[6]

Several interesting discoveries have emerged from laser-induced shock experiments on nanosecond time scales at Trident. Shocks along the ⟨100⟩ crystal directions in silicon show no evidence of plastic flow.[2] The stress at which plastic flow occurs on these time scales has been investigated for single crystals and polycrystalline foils of materials, including beryllium, iron, tantalum, nickel-titanium, nickel aluminide, and ruthenium aluminide. The results have contributed to the development of time-dependent plasticity models and of simulations with explicit treatment of the motion of dislocations.[4,7,8,9] In the rest of this article, we will review recent advances in dynamic loading by laser ablation and in TXD.

Dynamic Loading Induced by Laser Ablation

Shocks and other loading histories can be induced in samples of material by surface ablation resulting from the absorption of laser energy. At the start of the laser pulse, energy is deposited in the skin depth at the surface of the sample. Material at the surface ablates in the form of a plasma; subsequent laser energy is deposited in this plasma. Reaction and the plasma itself apply pressure to the remaining material in the sample, until the laser pulse ends and the plasma cloud dissipates (Figure 1).

A laser pulse of constant irradiance does not induce a constant pressure in the sample. We see a pressure spike in the first ~ 100 ps while the ablation plasma is established, followed by a period in which the plasma profile close to the sample is roughly constant and acts as a rocket. If a constant pressure shock is desired—necessary for accurate measurements of the EOS—then we must adjust the irradiance history of the laser pulse. At Trident, optical zone plate arrays are used to distribute the laser energy uniformly over a spot on the sample. For dynamic-materials work, we have mainly used a zone plate giving a 4-mm spot. At this scale, Trident can deliver irradiances up to ~ 10 PW/m^2, inducing pressures of up to several tens of gigapascals. For laser-pulse durations around 1 ns, the sample thickness is 10 to 500 μm, so the drive is safely one-dimensional over most of the area of the spot.

In nanosecond mode, the Trident laser pulse consists of 13 sequential elements, each 180 ps long, whose amplitude can be controlled independently. As well as being able to set the irradiance history to produce a constant pressure, we have also generated decaying shocks (analogous to the von Neumann spike or Taylor wave induced by detonation waves in chemical explosives) and isentropic compression waves (starting with a low irradiance and increasing

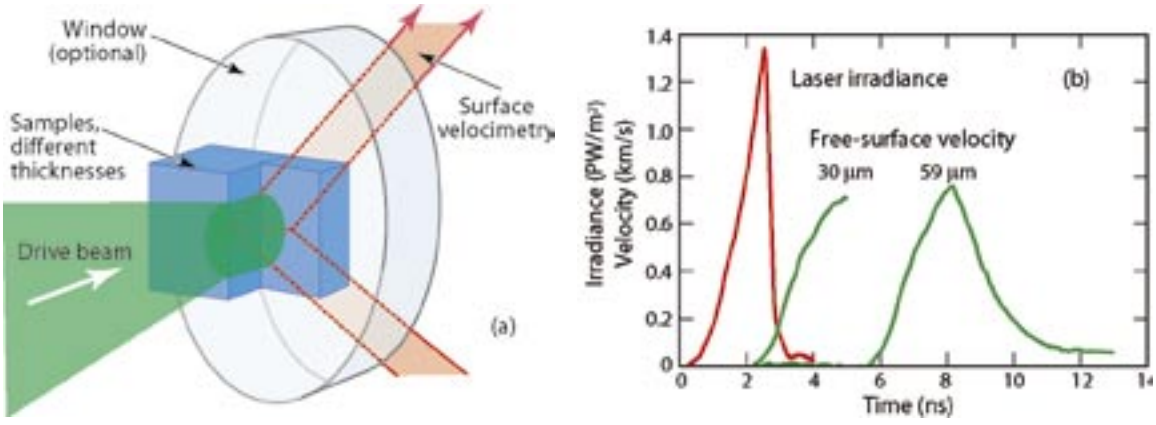

Figure 2. Schematic of side-by-side targets of different thickness used for laser-induced isentropic compression experiments (LICE) (a) and example results from Trident shot 15018 (silicon crystals) showing ramped laser pulse and smooth acceleration history at the surface of each sample (b).

gently to drive a smooth ramp wave through the sample). Isentropic compression experiments (ICE) driven by pulsed electrical power on microsecond time scales have been used to measure the EOS in beryllium and lead; we have used the laser-driven equivalent (with the unfortunate acronym of LICE) to generate ramp waves on nanosecond time scales in aluminum, silicon, iron, and tantalum (Figure 2).

Transient X-ray Diffraction

In TXD, a source of x-rays is used to infer the state of the crystal lattice by diffraction during the passage of a shock wave. We have used a laser-generated plasma as the x-ray source by focusing a beam delivering ~ 200 J in ~ 1 ns to a spot ~ 100 μm in diameter on a foil around 10 μm thick. For titanium and manganese foils, the resulting plasma emits predominantly helium-like line radiation (i.e., from atoms stripped of all but one electron) whose wavelengths are 2.61 and 2.006 Å, respectively—useful for experiments on a variety of materials. We have recorded the diffracted x-rays with two-dimensional time-integrating detectors (x-ray film and image plates) and one-dimensional time-resolving detectors (x-ray streak cameras). The coverage in terms of solid angle is typically quite small, so usually a particular small set of diffraction lines is followed as a function of drive pressure, rather than uniquely identifying a complete diffraction pattern from each experiment.

Previously, experiments have been performed on shocks in single-crystal samples, demonstrating the onset of plasticity and solid-solid phase transformations.[2,10] We have now performed some initial TXD experiments on dynamic melting in single crystals of gallium, which we use as a convenient melt prototype because its low melting temperature (29.8°C) makes it easier to distinguish the effects of melt from plasticity and phase transitions (Figure 3). Our ultimate application is beryllium for ICF capsules, where, in addition to plasticity and a possible solid-solid phase change, melt is expected to occur at ~ 150 GPa, requiring TXD to be performed over a wide range of diffraction angles.

We have also demonstrated time-resolved diffraction from rolled polycrystalline foils of beryllium, using a collimator so that only a small region of the sample was illuminated (Figure 4). For single crystals, the position on the sample surface at which diffraction occurs moves as the lattice is compressed. Polycrystal TXD allows a greater variety of samples to be used and also makes it easier to perform experiments at higher pressure, where the single-crystal diffraction point would move too far across the surface of the sample.

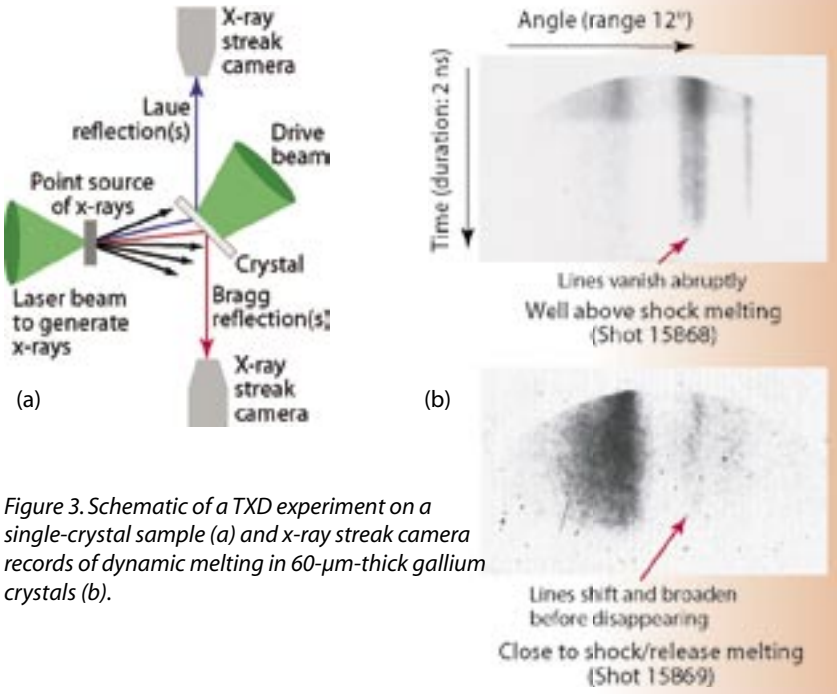

Figure 3. Schematic of a TXD experiment on a single-crystal sample (a) and x-ray streak camera records of dynamic melting in 60-μm-thick gallium crystals (b).

Conclusion

Dynamic loading by laser ablation has provided valuable insights into the detailed response—plasticity and phase changes—of materials on nanosecond time scales and pressures to tens of gigapascals. This regime is important in the development of improved material models for weapons and ICF applications. The use of lasers has made it easier to develop new diagnostic techniques, providing subnanosecond temporal resolution and greater ease in synchronizing the measurement with the drive. We expect to develop these techniques further and apply them to a wider range of materials, working more closely with the development of advanced, physically based models.

References

1. A.V. Bushman, G.I. Kanel, A.L. Ni *et al.*, *Intense Dynamic Loading of Condensed Matter* (Taylor and Francis, London, 1993).
2. A. Loveridge-Smith, A. Allen, J. Belak *et al.*, "Anomalous elastic response of silicon to uniaxial shock compression on nanosecond time scales," *Physical Review Letters* **86**(11), 2349–2352 (2001).

3. M.A. Meyers, F. Gregori, B. K. Kad *et al.*, "Plastic deformation in laser-induced shock compression of monocrystalline copper," in *Shock Compression of Compressed Matter–2001*, M.D. Furnish, N.N. Thadhani, and Y. Horie, Eds. (American Institute of Physics, New York, 2002), AIP Conference Proceedings 620, pp. 619–622.
4. D.C. Swift, D.L. Paisley, G.A. Kyrala *et al.*, "Simultaneous VISAR and TXD measurements on shocks in beryllium crystals," in *Shock Compression of Compressed Matter–2001*, M.D. Furnish, N.N. Thadhani, and Y. Horie, Eds. (American Institute of Physics, New York, 2002), AIP Conference Proceedings 620, pp. 1192–1195.
5. S.R. Greenfield, D.L. Paisley, and A.C. Koskelo, "Transient interferometric studies of shocked bicrystals," in *Proceedings of the APS Topical Conference on Shock Compression of Condensed Matter*, held in Portland, Oregon, July 21–25, 2003 (to appear).
6. P. Peralta, E. Loomis, K.J. McClellan *et al.*, "Characterization of laser-driven shocked NiAl monocrystals and bicrystals," in *Proceedings of the APS Topical Conference on Shock Compression of Condensed Matter*, held in Portland, Oregon, July 21–25, 2003 (to appear).
7. R.E. Hackenberg, D.C. Swift, J.C. Cooley *et al.*, "Phase changes in Ni-Ti under shock loading," in *Proceedings of the International Workshop on New Models and Hydrocodes for Shock Wave Processes in Condensed Matter*, Edinburgh, Scotland, May 19–24, 2002 (to appear).
8. K.J. McClellan, D.C. Swift, D.L. Paisley *et al.*, "Dynamic properties of nickel-aluminum alloy," in *Proceedings of the APS Topical Conference on Shock Compression of Condensed Matter*, held in Portland, Oregon, July 21–25, 2003 (to appear).
9. D.C. Swift, D.L. Paisley, A. Forsman *et al.*, "Dynamic flow stress and polymorphism in shocks induced by laser irradiation," in *Proceedings of the 5th Symposium on High Dynamic Pressures*, held in St. Malo, France, June 23–27, 2003 (to appear).
10. D.C. Swift, G.J. Ackland, A. Hauer *et al.*, "First-principles equations of state for simulations of shock waves in silicon," *Physical Review B* **64**, 214107 (2001).

Acknowledgment

Our team would like to recognize the contribution of the staff of the Trident laser facility in performing these experiments. We would also like to recognize the ICF and Science and Technology Base Program Offices for supporting this work.

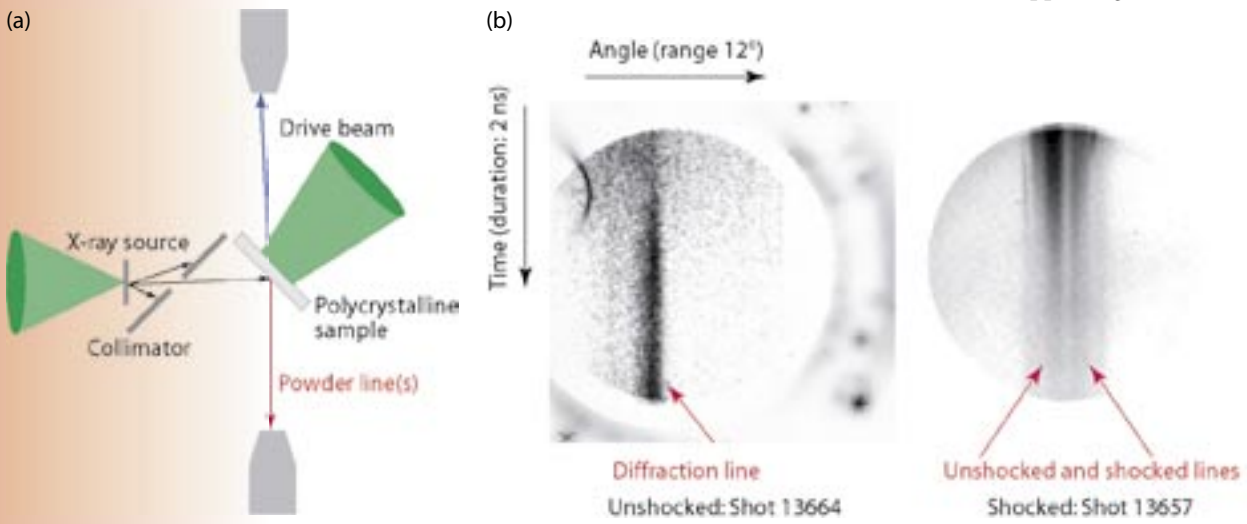

Figure 4. Schematic of a TDX experiment on a polycrystalline sample and x-ray streak-camera data demonstrating powder lines for 125-μm-thick beryllium foils (a). The shock in Shot 13657 was ~ 20 GPa. The width of the diffraction lines was dominated by the aperture in the collimator (b).

For more information, contact Damian Swift at 505-667-1279, dswift@lanl.gov.

pRad VISAR: An Interferometer-Based Optical Diagnostic for Proton Radiography

D. Tupa (P-25), D.A. Clark, O.F. Garcia, B.J. Hollander, D.B. Holtkamp (P-22)

One method to determine the velocity of a moving surface is to measure the Doppler-shifted frequency of light reflected off that surface. A sensitive measurement of frequency can be made with an interferometer. One specific interferometer configuration for such a measurement was developed at SNL and LANL and is called VISAR, for velocity interferometer system for any reflector.[1,2] We have developed and implemented a VISAR capable of measuring up to seven points simultaneously for the LANL pRad facility. In this article, we briefly describe how our VISAR works and how it is used to supplement proton radiographs.

How VISAR Works

A VISAR is diagrammed in Figure 1. After reflecting off the surface in question, light enters the interferometer from the fiber-optic input on the left-hand side (LHS) and is incident on a 50/50 beamsplitter. Half the light is reflected off the beamsplitter, the LHS mirror, and is incident on the beamsplitter again. The other half of the light traverses the right-hand side (RHS) of the interferometer. For imaging, the RHS is optically equivalent to the LHS despite having an optically flat element, an etalon, in the beam path. The etalon induces a frequency-dependent phase shift between the light traversing either side of the interferometer. After the light is recombined at the beamsplitter, the relative phase shift is measured by keeping count of the Michelson-type fringes through the fiber-coupled output of the device; the fringes are manifested as modulations in the light intensity. The light frequency can be deduced from this relative phase shift. A single fiber-coupled output would suffice for a measurement, but the eighth-waveplate, output polarizing beamsplitters, and additional outputs allow for greater precision throughout the measurement range and calibration against light-intensity variations and unwanted scattered light.[2]

In addition to allowing for measurements with reflected light from diffuse surfaces, having each side of the interferometer optically equivalent allows measurements of velocity of different points at the same time. Rather than a single optical fiber for input, a bundle of seven fibers is used (Figure 2).

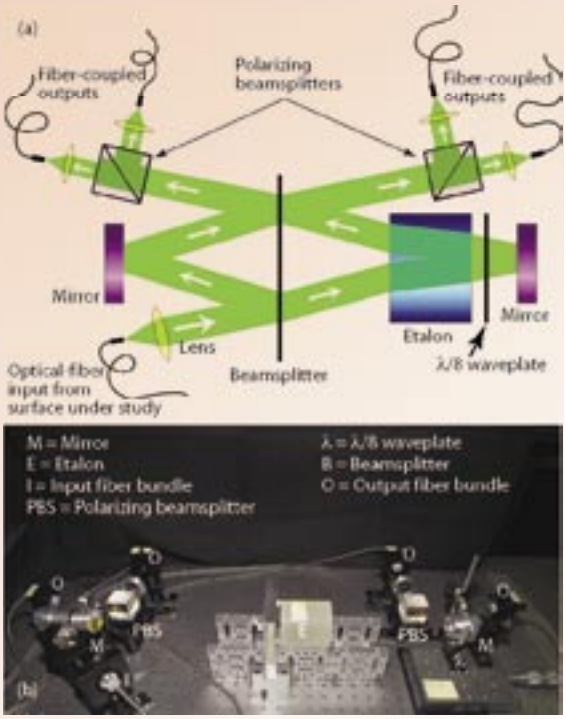

Figure 1. (a) Schematic diagram and (b) photo of the pRad VISAR. Details are given in the text.

Figure 2. Photo of the input fiber bundle on which the ends of the seven individual fibers can be seen. The diameter of the hole for each fiber is 370 μm.

Each fiber in the bundle carries light reflected from a different test point on the experiment. The input bundle is carefully imaged onto four identical fiber bundles at the four output arms of the interferometer. The four output intensities of each of the seven test points can then be recorded simultaneously on a streak camera.

The streak camera records data with a 1,000- × 1,000-pixel CCD with 15 ns/pixel, typically. The noise on the velocity measurement is usually below 40 m/s. The breakout time, the time of a sudden change in surface velocity caused by shock, can usually be determined with an instrumental precision of ± 30 ns. In parallel with the streak camera, the light intensities from at least one point can also be recorded with photomultipliers and a digitizing oscilloscope. Typical sample time for the scope is 2 ns.

Integrating VISAR with pRad

The pRad dome (located in Area C at LANSCE) environment presents challenges for setting up a VISAR system. Hazards such as radiation and high explosives are integral to the facility, so the VISAR light source, optics, and data-acquisition equipment must be located outside the pRad dome. Conversely, the VISAR must be operated in such a way that workers are not endangered by its high-power laser.

A schematic overview of how the VISAR equipment is integrated into the pRad area is shown in Figure 3. A separate, interlocked room houses the VISAR equipment and controls. The light for the VISAR comes from a laser producing 10 W at 532 nm. After passing through an attenuator and a fast switch, the laser beam enters a seven-way switchyard, where it can be divided into seven beamlets of arbitrary intensity. Each of the seven beamlets is coupled into a fiber-optic cable that carries the light 100 m to the pRad dome. A vacuum feed-through connects this supply fiber to the VISAR probe. The VISAR probe is a compact optical device placed in the vacuum chamber with the test object. The probe (Figure 4)

- directs the collimated laser light to the surface of the test object,
- gathers the light that is reflected back, and
- couples it back into a second fiber of the vacuum feed-through.

The output of the probe is returned to the VISAR room, where it is directed into one of the seven interferometer input fibers.

Experimental Results

VISAR surface-velocity measurements and proton radiographs complement each other well. Proton radiographs reveal three-dimensional views of the total volume of an object during a dynamic event but do so at discrete intervals of 3 μs, typically, and the images are integrated over 50 ns. VISAR can only reveal the velocity of the exterior surface of the object but provides a relatively continuous record with measurements every 2–15 ns.

Experiments to study high-explosive-induced damage and spall[3,4] in selected metals demonstrate how VISAR data can enhance observations of dynamic experiments. These experiments study the behavior of metals when the free surface reflects a Taylor wave generated by high explosives. Figure 5 is a diagram of such experiments performed in conjunction with pRad operations.

Some results of these experiments, showing the velocity of the metal surface as measured by the VISAR, are shown in Figure 6. The terminal velocity, velocity pullback, shock breakout, and ringing period of the surface can be seen in the VISAR data. This information yields independent measurements of parameters such as the spall strength of the material and thickness of the first spall/damage layer.

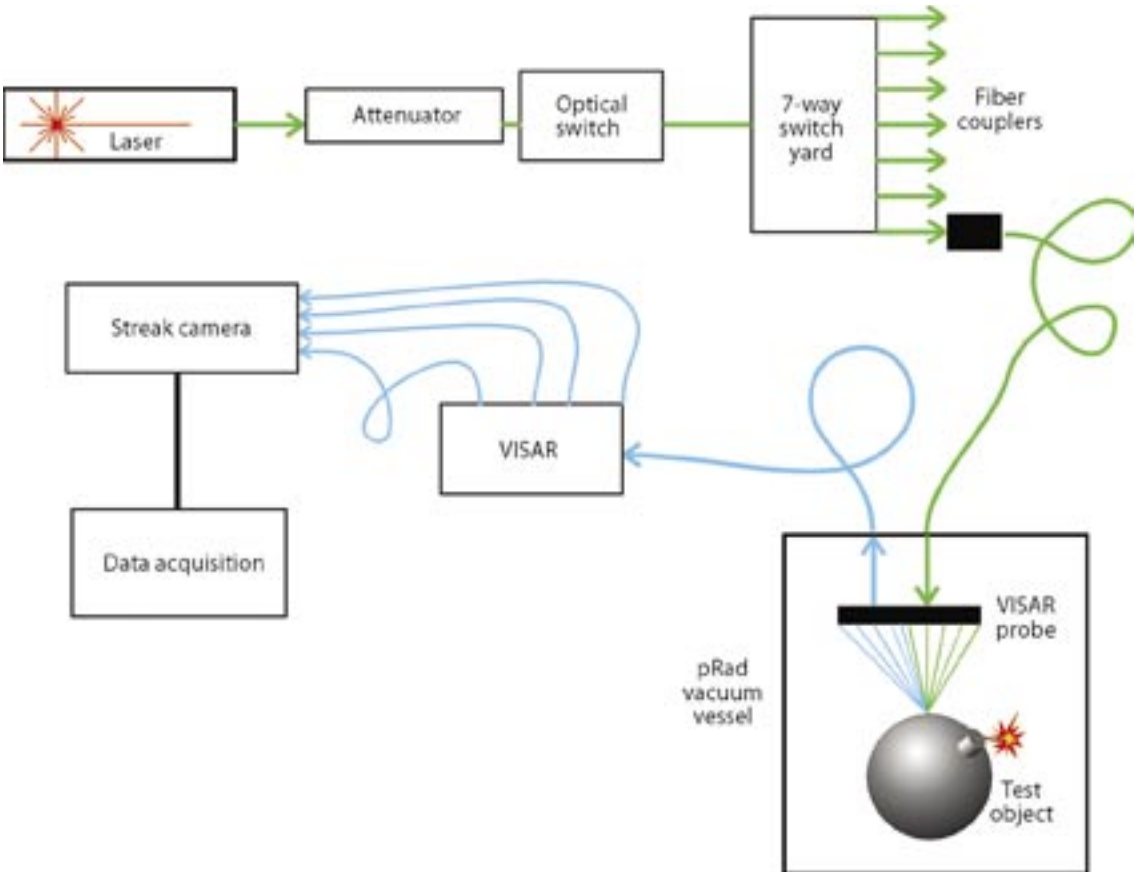

Figure 3. Schematic of the VISAR measurement apparatus, as used for pRad.

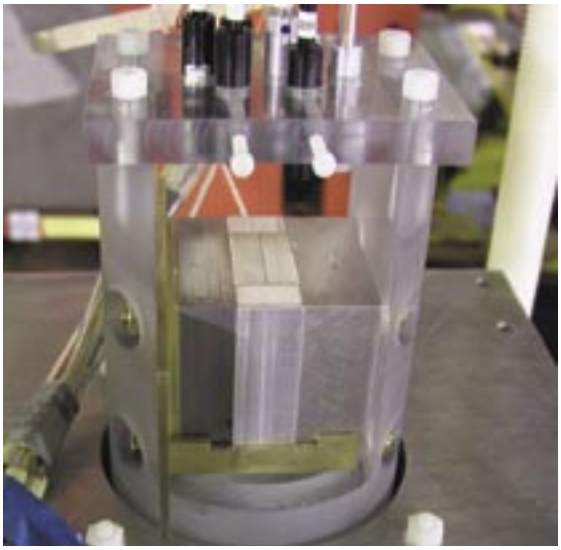

Figure 4. Seven VISAR probes aligned onto a pRad experiment. The black and metallic cylinders held by the upper Lucite block are the probes. Seven points of green light on the surface of the test object are from the alignment laser light coming through the probes; scattered light from each spot is gathered by the respective probe to be analyzed by the VISAR interferometer.

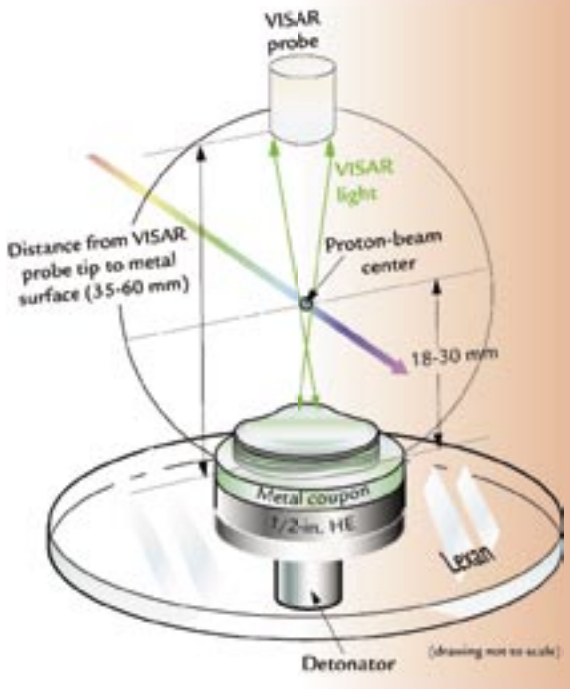

Figure 5. Diagram of high-explosive spall/damage experiment. The composition and thickness of the metal cylinder, or coupon, varies for different experiments.

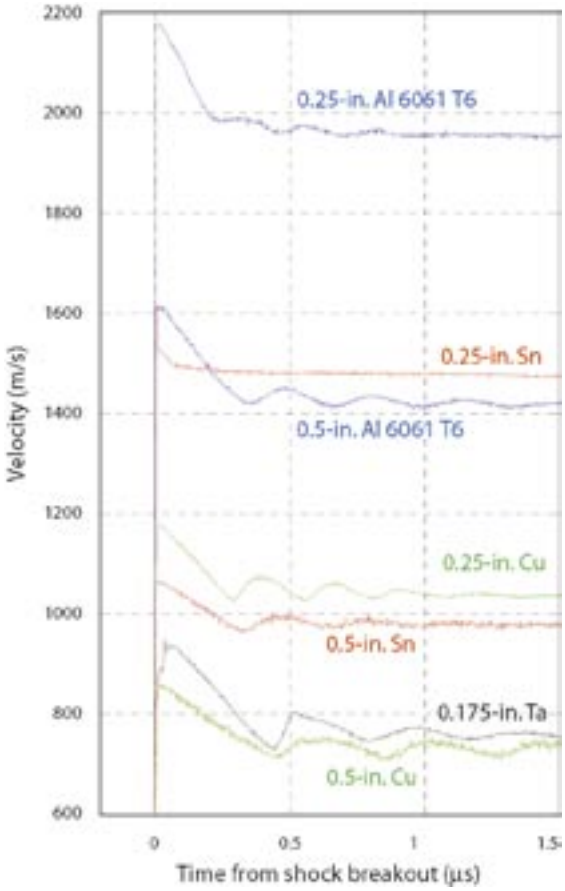

Figure 6. VISAR measurements of surface velocity from several pRad experiments. Results are shown for differing thicknesses of 6061-T6 aluminum (blue), tin (red), copper (green), and tantalum (black). Zero time is adjusted for breakout at the same time for each experiment. The entire time scale of the graph is < 3 µs, the typical spacing between pRad images.

Conclusion

A VISAR system has been installed in pRad to measure the surface velocity of test objects during dynamic experiments. The system has been upgraded to allow measurements of up to seven points on the surface simultaneously. The system has been used for over a dozen experiments in the last year at pRad. The pRad VISAR is ready to be available upon request to users at pRad to supplement the information learned in their experiments.

References

1. L.M. Barker and R.E. Hollenbach, "Laser interferometer for measuring high velocities of any reflecting surface," *Journal of Applied Physics* **43**(11), 4669–4675 (1972).
2. W.F. Hemsing, "Velocity sensing interferometer (VISAR) modification," *Review of Scientific Instruments* **50**(1), 73–78 (1979).
3. D.B. Holtkamp D.A. Clark, I.A. Garcia *et al.*, "Development of a non-radiographic spall and damage diagnostic," in *Proceedings of the 2003 Conference of Shock Compression of Condensed Matter*, M.D. Furnish, Ed. (to appear in April 2004).
4. D.B. Holtkamp, "High explosive-induced damage and spall in selected materials studied with proton radiography," in *Proceedings of the 2003 Conference of Shock Compression of Condensed Matter*, M.D. Furnish, Ed. (to appear in April 2004).

Acknowledgment

The experimental program at pRad is operated by the Proton Radiography Collaboration, which staged and executed all the shots performed with pRad VISAR, including those summarized in Figure 6. For VISAR operations, Karen A. Esquibel (P-22) provided technical assistance, Paul Nedrow (P-23) installed and operated the streak camera, and Anthony J. Zukaitis (Bechtel-Nevada) assisted with data analysis. Funding for this work came from the Advanced Radiography Program Element (Campaign 3) of the Weapons Development Program.

For further information, contact Dale Tupa at 505-665-1820, tupa@lanl.gov.

Temperature of Shocked Materials

V.W. Yuan, J.D. Bowman, G.L. Morgan (P-23), D.J. Funk, D.G. Thompson (DX-2), R.A. Pelak, L.M. Hull (DX-3), C.E. Ragan (X-5), J.E. Hammerberg (X-7), M.S. Shaw (T-14)

Neutron resonance spectroscopy (NRS) uses the Doppler broadening of neutron resonances to determine the temperature in samples undergoing dynamic loading. This technique has emerged as a unique method for making temperature measurements in the field of shockwave and high-explosive physics—as such, it can be applied to Science-Based Stockpile Stewardship and the Weapons Program. NRS can determine temperatures on very short time scales (1 μs or less) and has been used to determine the internal volume temperature in shocked molybdenum and in explosively driven metal jets. In 2003, the NRS team began the first experiments to measure the temperature behind the burn front of detonating high explosives; measurements of this burn temperature have never before been made *in situ*. For many materials of interest, dynamic temperature measurements appear possible at many attainable conditions on the EOS surface.

Why Neutrons?

NRS experiments use low-energy neutrons because these minimally perturbing probes possess advantages over other available temperature diagnostics. First, optical opacity or ancillary light emissions do not limit the technique because photons are not detected. Second, the technique uses small amounts of resonant tags, or dopants, that can be localized in the samples being studied. For a given experiment, the type of dopant and quantity (about 1 at. %) is selected so that it causes minimal perturbations to the dynamically loaded sample. The localization of the doped region allows us to make temperature measurements in a steady shock region internal to the sample rather than at a free surface or visible interface where rarefactions can alter the state being characterized.

What is a Neutron Resonance?

When a beam of neutrons passes through a sample of atomic weight A, those neutrons possessing certain resonant energies (usually in the epithermal region below a few hundred eV) can be captured by sample nuclei to form an excited state in the "compound nucleus" of atomic weight A+1. The capture interaction removes neutrons from the beam passing through the sample. A detector placed downstream of the sample measures the neutron flux as a function of the time when the neutrons arrive; there are dips (Figure 1) in the observed spectra at the energies at which the compound nuclei were formed. The depths of the resonances and their energies are unique to the materials traversed by the neutrons. NRS experiments can take advantage of this uniqueness to localize temperature measurements in space by inserting a dopant that resides only in the region of interest. The shapes of these resonances depend on both intrinsic resonance properties and on the Doppler broadening produced by the motion of atoms in the target sample. By measuring the amount of broadening produced, NRS determines the temperature of the sample.

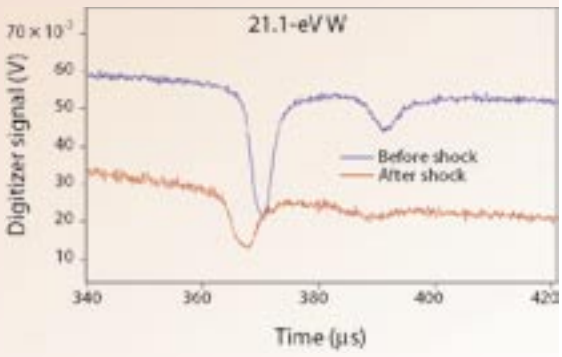

Figure 1. Resonances at 21 eV and 18 eV in the transmitted neutron flux through an isotopically enriched ^{182}W sample before and after the material is shocked. The two curves show the comparative broadening of the resonances, as well as the shifts in resonance positions.

LANSCE Accelerator Provides an Intense Source of Neutrons

Obtaining the necessary statistics for accurate NRS temperature measurements requires a copious source of epithermal neutrons in a single pulse. The linear accelerator at LANSCE produces 800-MeV protons that are loaded into the Proton Storage Ring where they are accumulated and then released as a short, intensified beam pulse. (Each pulse contains about 30 trillion protons.) The intense proton pulse is directed at a uranium spallation target and produces many high-energy neutrons upon striking the target. These high-energy neutrons then bounce around in a polyethylene moderator where they slow down to epithermal energies and emerge into the NRS secondary beam line. With this special setup, NRS achieves neutron brightness levels an order of magnitude higher than is presently available at the main LANSCE production target.

A fast temperature "snapshot" is required to study dynamically loaded systems. For instance, to measure the temperature after the passage of a shockwave, the measurement must be recorded after the sample is fully shocked but before any rarefactions return from the front, rear, or side surfaces. The time window for measuring the unreleased temperature in a shocked metal is about 1 μs (Figure 2). The time resolution of the NRS measurement is determined by the spread in transit times of resonant neutrons traversing the sample. In the Blue Room at LANSCE, the sample can be placed at a short distance (within 1 m) from the moderator, and fast time resolutions of several hundred nanoseconds are achievable.

Figure 2. Rendering of an NRS experiment to measure temperature in a shocked metal. (a) An explosively launched aluminum flyer initiates the shock in a molybdenum target, which contains a region doped with ^{182}W. Neutrons probe the doped region after the passage of the shock wave but before the return of rarefactions. Figure 2(b) is a view inside the target chamber used in the NRS experiment at LANSCE.

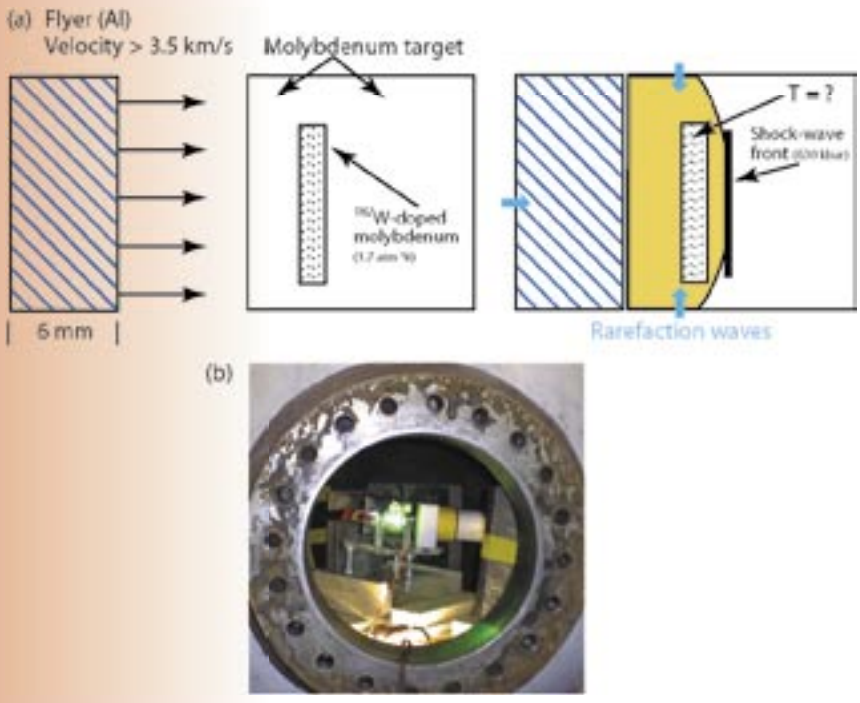

Temperature Behind the Passage of a Shock Wave in Molybdenum

The NRS experimental effort with highest priority is the measurement of the temperature behind a strong shock in a metal. This type of measurement provides a means for testing various EOS models. NRS is currently the only technique capable of measuring the internal temperature without significantly altering the shocked state. The NRS team has performed temperature measurements in molybdenum within 1 μs of the passage of a shock wave through the sample. Within the constraints imposed by the high-explosive load limit in the containment vessel, the sample size, geometry, and location of the doped region in the metal were selected to maximize the time between passage of the shock and the appearance of rarefaction waves at the doped region. A preliminary analysis of the NRS data indicates that two shots provided temperatures of 785 ± 59 K and 908 ± 35 K for particle velocities of 0.90 and 0.96 km/s, respectively. Figure 3 shows that both measured temperatures are higher than those presently predicted by the best SESAME EOS[1] for molybdenum (SESAME 2984).

For safety reasons, the dynamic shots are fired at an angle to the neutron beam so as to prevent penetration of the containment vessel windows by shrapnel. Because of this tilt angle, the beam does not arrive simultaneously at all parts of the doped layer. The nonsimultaneity of arrival can alter the perceived temperature; we are currently modeling the effect that the tilt of the sample has on the derived temperature. So far, the effect of the tilt is too small to account for the difference between our experimental results and theory. The NRS team is currently working on design changes for future experiments that would reduce the hydrodynamic effects introduced by the sample tilt. A review of the NRS program by the Campaign 2 management encouraged EOS studies in metals as a high priority. In the latter part of the LANSCE 2003–2004 run cycle, we plan to perform additional experiments on molybdenum and/or other metals.

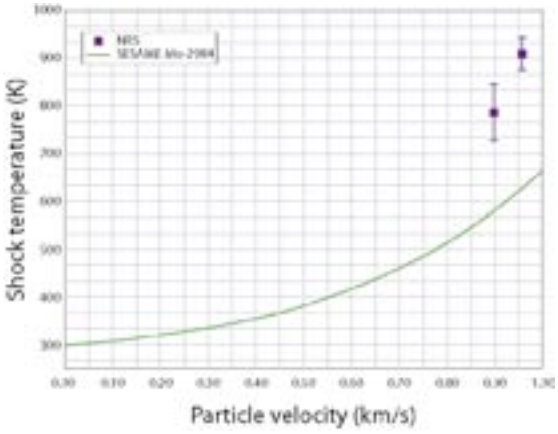

Figure 3. Shock temperature values extracted from NRS data are compared to theoretical values calculated using SESAME 2984 EOS. Temperatures are higher than the predicted values.

Measurement of the Temperature Behind the Burn Front of Detonating High Explosives

In a second experimental thrust, we measured the temperature behind the burn front of a high explosive detonated by a 6-mm-thick aluminum flyer plate. (The setup was similar to the one used in the shocked-metal experiment described above.) Through the use of a flyer plate, we can support the pressure behind the detonation front at a value just below the Chapman-Jouguet (CJ) point for the explosive (Figure 4). An NRS determination of the temperature inside detonation products of high explosives would fill a major gap in the characterization of its EOS. The largest uncertainty in theoretical modeling comes from the chemical equilibrium composition. Calculations by Sam Shaw (T-14) indicate that a shift from the combination of CO_2 and carbon in the products to CO can reduce the released energy by around 25%. Shaw calculates the corresponding shift in temperature to be around 1,000 K. This very strong correlation of the temperature with the composition is what makes the NRS measurements so useful. Several thermodynamic methods using potential energies exist for treating the EOS of high-explosive products, and these can be calibrated against experimental data. Additional calculations confirm that the WO_3 dopant has negligible effect on the high-explosive temperature. The fine-tuning of Shaw's model against NRS temperature measurements would greatly narrow the allowed parameter space and provide insight into the EOS of the high explosive.

The initial dynamic high-explosive EOS experiment performed by the NRS team did not result in a valid temperature measurement because of unanticipated dopant-clumping in the sample. Clumping can result in non-uniform thickness that distorts the extracted temperature; if the clumps are large enough, the temperature will not equilibrate within a clump. A subsequent NRS dynamic experiment used a new method of high-explosive formulation that was designed to reduce the clumping of the dopant in the high-explosive samples. Analysis indicates that the new formulation significantly reduced the clumping within the sample but did not completely eliminate it. The NRS measurement also indicated a particle velocity nearly one-half that predicted, but unfortunately the independent VISAR velocity measurement was lost because the VISAR optical fiber was damaged prematurely by the explosive. For future experiments, we will use a formulation of doped high explosive that incorporates nanoparticle tungsten-oxide dopant to further reduce non-uniformity and clumping. However, further shots may not take place until other higher-priority experiments are completed.

Measurement of the Temperature at a Sliding Interface at High Pressures and Velocities

Another challenge that the NRS team plans to address is determining the properties of a shocked metallic interface. One such interface of great interest exists between two materials possessing significantly different shock speeds. If a shock is initiated in both at the same time (Figure 5), the shock on one side of the interface will outrun the shock on the other side, causing the two materials to slide relative to each other at high velocity while experiencing a large normal force caused by the high-pressure shock. To date, there are no experimental data on the temperature rise at a compressed, sliding interface at high pressures and velocities. A constitutive model of the tangential

Figure 4. (a) This rendering depicts an unsupported detonation. (b) This rendering depicts how an aluminum flyer plate in the NRS experiment supports the pressure behind a detonation front at a value just below the CJ point for the explosive.

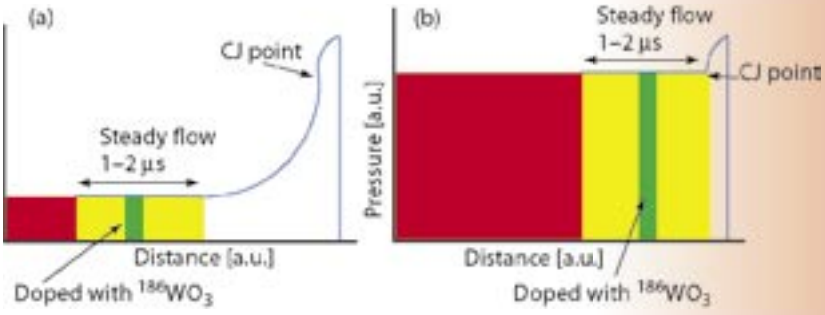

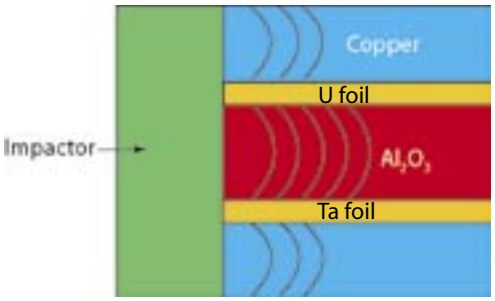

Figure 5. Schematic showing shock in sapphire (Al_2O_3) outrunning the shock in the adjoining copper. The neutron beam is passed through the sandwich, and resonances in Ta and U foils located at the Al_2O_3/Cu interfaces provide temperature data.

force as a function of pressure, temperature, sliding velocity, and the state of interfacial deformation at short times ($t < 50$ μs) was constructed.[2-4] However, there has been little in the way of experimental data to guide models that are important to the code development efforts of X Division. Measurements of the interfacial temperature will provide bounds on the parameters in the models and their uncertainties.

Our first NRS friction experiment will measure the temperature under dynamic conditions. The sample will consist of a sandwich comprised of an Al_2O_3 slab between slabs of copper (each slab being 2 cm thick). In addition, thin foils (50 to 100 μm thick) will be placed at the interfaces—a tantalum foil at one interface and a uranium foil at the other. An explosively launched aluminum flyer plate traveling parallel to the interfacial planes will impact the sandwich at about 2.5 km/s. Because shock in the Al_2O_3 travels much faster than the shock in the copper, a steady sliding state of about 1 cm in length should be achieved for a little over 1 μs. The shock pressure should be about 200 kbar, and relative interfacial velocities between the Al_2O_3 and foils should be about 0.5 km/s. The neutron beam will pass through the target while the temperature is elevated from the frictional heating. The temperature rise in the foils should be between 100 and 1,000 K, depending on the magnitude of the frictional force; by measuring the temperature, we should gain knowledge of the frictional force. There are resonance lines in tantalum and uranium at 39 eV and 37 eV, respectively, and they are separated enough in energy for temperature measurements to be possible at the two interfaces in the same experiment.

References

1. B.I. Bennett, J.D. Johnson, G.I. Kerley, and G.T. Rood, Los Alamos Scientific Laboratory report LASL-7130 (unpublished); Los Alamos Scientific Laboratory brochure LASL-79-62 (unpublished); Equation-of-State and Opacity Group, Los Alamos National Laboratory brochure LALP-83-4 (unpublished); S.P. Lyon and J.D. Johnson (Eds.), "SESAME, the Los Alamos National Laboratory equation of state database," Los Alamos National Laboratory report LA-UR-92-3407 (1992).
2. J.E. Hammerberg *et al.*, "Nonlinear dynamics and the problem of slip at material interfaces," *Physica D* **123**, 330–340 (1998).
3. J. Röder *et al.*, "Multichain Frenkel-Kontorova model for interfacial slip," *Physical Review B* **57**, 2759–2766 (1998).
4. J. Röder *et al.*, "Dry friction: modeling and energy flow," *Physica D* **142**, 306–316 (2000).

Acknowledgment

We would like to acknowledge those individuals without whose efforts and help this work could not have been performed. Ron Rabie, now retired, has been an integral member of the collaboration and a driving force. We are indebted to the DX firing crews who helped setup and fire our explosive shots, in particular, Howard Stacy, Pat Quintana, Don Murk, Robert Lopez, Steve Dennison, Fidel Martinez, Joe Bainbridge, and Vern Lawrence. The work of Bruce Takala, the Blue-Room Experimental Area Manager and LANSCE-3 technicians Greg Chaparro and Lloyd Hunt are essential to the setting up of our apparatus in the Blue Room, as is Gil Peralta from P-23. We have had valuable discussions with Carl Greeff of T-1, and he has provided calculations of predicted temperatures relevant to the shocked metal experiment. Finally, the LANSCE-6 operations crew provided invaluable assistance in tuning and delivering the sole-use proton beam that is absolutely necessary for carrying out these experiments. The NRS work has been funded by Campaign 2 of the DOE Defense Programs. Excursions into the studies of metal jets have received funding from a DOE/DoD memorandum of understanding.

For more information, contact Vincent Yuan at 505-667-3939, vyuan@lanl.gov.

Ejecta Density Measurements Using Soft X-ray Radiography

D.S. Sorenson, N.S.P. King, K. Kwiatkowski, I. Campbell (P-23), R.T. Olson (P-22), J.L. Romero (University of California, Davis)

Soft x-ray imaging has been developed and used for measuring ejecta density distributions from shock-loaded metals. Ejecta are metal particles (solid or liquid) that are emitted from a shock-loaded surface. Over the years, we have developed an electronic imaging system capable of recording up to four images. In particular, we have focused on three main areas: multiframe camera systems, image-relay systems, and scintillators. Our system is currently capable of measuring ejecta densities down to 0.5 mg/cm^2 over a 50-mm^2 field of view using lutetium oxyorthosilicate/yttrium oxyorthosilicate scintillators (200–300 μm thick). The x-ray sources typically give 15 mrad at 1 m with a spot size of 1.5 mm. We can obtain typical interframe times of hundreds of nanoseconds to many microseconds. Images formed on the scintillator are relayed through coherent bundles and connecting-fiber-optic reducers over a distance of about 3 m.

We are also developing various models of our experiments using Monte Carlo methods. These models enable us to accurately calculate plutonium transmission versus areal densities, which we use to calibrate our data. Figure 1 shows an example of data and a simulation for a range of metal foils. We expect to continue improving the soft x-ray imaging system and the simulation models to allow us to more accurately determine ejecta density distributions.

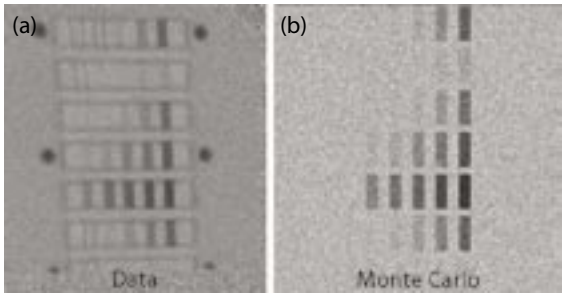

Figure 1. Comparison between data (a) and a Monte Carlo prediction (b).

Cross Validation of Ejecta-Areal-Density Measurement Techniques

R.T. Olson (P-22), W.T. Buttler (P-23), W.W. Anderson (DX-2)

Ejecta-diagnostic-development experiments are being performed as a collaborative effort between P and DX Divisions. These experiments use piezoelectric pins, Asay foils, and x-ray radiography to simultaneously measure the ejecta areal density generated by a planar shock from the surface of a tin gas-gun target. Each measurement technique measures a different physical quantity that can be related to the ejecta areal density. The piezoelectric pins generate current as ejecta imparts a time-varying force to a lead-zirconate-titanate (PZT) ceramic material. The Asay foil velocity is recorded as ejecta inelastically collides with and transfers momentum to a thin foil. X-ray flux through the ejecta cloud is attenuated according to the type of ejecta material and its density. The data acquired by each diagnostic technique are then independently analyzed and compared to cross-validate the precision and accuracy of each technique. Experiments performed thus far indicated that the Asay foil and x-ray radiographic techniques provide areal-density measurements that agree to within ~ 15% of one another. The PZT pins have recorded areal densities that range from identical to a factor of three higher than the other techniques. Currently, additional experiments are being conducted to understand the reason behind this discrepancy.

Surface-Temperature Measurements Under Shock Compression

A.W. Obst, K. Boboridis, J.R. Payton, A. Seifter, W.S. Vogan (P-23)

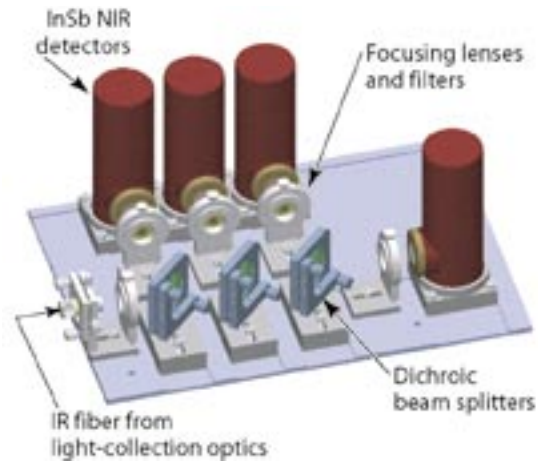

Figure 2. Rendering of an NIR pyrometer developed by members of P-23. Light incident from the left is wavelength split at each of the three dichroic beamsplitters. The four InSb NIR detectors then collect the light.

The accurate measurement of the temperature of shock-compressed materials is of great interest in high-pressure physics. Shock-physics experiments serve as a primary diagnostic in constraining the EOS of materials and in determining the state of ejecta and spallation from these surfaces. Shock techniques at LANL include the use of laser ablation at the Trident laser facility, gas guns at Ancho Canyon, and high-explosive Forrest flyers at TA-40, Chamber 8. We use high-speed, time-resolved, multi-wavelength near-infrared (NIR) surface pyrometry to measure shock temperatures from 400 K to 1,500 K. The detector unit of an NIR pyrometer developed by P-23 is shown in Figure 2. This instrument was calibrated at the National Institute of Standards and Technology (NIST) in Gaithersburg, MD.

Inferring the thermodynamic or true surface temperature from blackbody radiance-temperature measurements requires a knowledge of both the static and dynamic emittance, or equivalently emissivity, of materials under shock compression—both as a function of wavelength and temperature. Toward this end, we are developing a number of surface-study diagnostics, including high-speed laser NIR polarimetry; integrating-sphere reflectometry; and, for absolute calibration purposes, a pulse-heating system. The first two surface diagnostics have been built and are operational, whereas the pulse-heating system is under construction. A further EOS constraint is provided by comparing surface and volume temperatures, where the latter is obtained from NRS. The NRS high-explosive Forrest flyer experiments were done at LANSCE, whereas the comparative surface high-explosive Forrest flyer measurements are being done at TA-40, Chamber 8.

Fundamental Properties of Beryllium for ICF Applications

J.A. Cobble, D. Swift, T. Tierney (P-24), A. Nobile, B. Day (MST-7), D. Tubbs, N. Hoffman (X-1)

P-24 is actively engaged in a set of qualification experiments for beryllium as an ablator material for radiation-driven ICF. For a successful fuel implosion, among other requirements, the drive must be extremely uniform. This is where questions concerning beryllium arise. Although its strength and conductivity exceed that of alternate ablator materials, its structure is anisotropic. During that time in the implosion before the beryllium melts, this anisotropy is believed to drive hydrodynamic instabilities which can, in principle, destroy the target before ignition occurs. Understanding the anisotropy is complicated by the grain structure of the beryllium. For larger grains, this problem is aggravated, while for small enough grains, the inhomogeneities are expected to "average out." We must know the behaviors of these options for specifying a successful target design that we can fabricate for a reasonable cost.

We have begun experiments at the Omega laser at the University of Rochester to investigate the microstructure of beryllium and its role in Rayleigh-Taylor hydrodynamic instabilities. During the summer of 2003, we drove machined sinusoidal perturbations in planar beryllium samples with x-ray radiation from laser-driven hohlraums. The goal was twofold: to develop diagnostic techniques with the aim of observing the growth rate of instabilities caused by the beryllium microstructure and to develop a radiation-drive environment similar to that expected in the first few nanoseconds of requisite laser drive at NIF now under construction at Lawrence Livermore National Laboratory (LLNL). The initial Omega experiments provided data that encourage us to continue the research. P-24 is closely allied with theoretical physicists in X-1 who model the experiments for comparison with the Omega results.

High-Speed Pyrometry Measurement of Shocked Tin and Lead

D. Partouche-Sebban, R.R. Bartsch, D.B. Holtkamp, P. Rodriguez, J.B. Stone, L.J. Tabaka, D.T. Westley (P-22), F.G. Abeyta, W.W. Anderson, M.E. Byers, F.J. Cherne, D. Dennis, J.S. Esparza, C.M. Fowler, R.S. Hixson, P.A. Rigg, D.L. Shampine (DX-2)

P and DX Divisions have recently undertaken a study of the Hugoniot and melt curves of tin and lead in the pressure-temperature diagram up to about 60 GPa in pressure. In most shock experiments, the sample temperature needs to be measured in less than a microsecond. Currently, high-speed optical pyrometry seems to be the best way to perform this measurement. This is still a challenge for any metal because a strong optical background is generally present in such experiments and needs to be totally eliminated. Moreover, when studying metals, pyrometry accuracy is mainly limited by the fact that the emissivity of the shock-loaded sample is not known accurately. As a result, we carefully select the pyrometer wavelengths in order to minimize the effect of emissivity uncertainty on these experiments.

The preliminary results on tin are promising and supplement previous data to confirm that the Hugoniot curve of tin is somewhat higher than expected. Reflectivity diagnostics are also fielded to obtain data on the sample surface emissivity during the experiment in order to both improve the accuracy on temperature and perhaps to detect phase transitions.

The experimental program on lead will begin in early 2004. In particular, several kinds of transparent windows (LiF, PMMA, and sapphire) will be used to cover a large part of the melt curve in the vicinity of where it coincides with the Hugoniot curve.

Subcritical Experiment Diagnostics

D.A. Clark, C.M. Frankle, D.B. Holtkamp, P. Rodriguez, J.R. Smith, L.J. Tabaka, D.T. Westley (P-22), with significant collaboration from other LANL groups, Sandia National Laboratories, Bechtel Nevada, and the Atomic Weapons Establishment

In the summer of 2002, the SCEs, Mario and Rocco, and two confirmatory shots were fired in the U1a complex at NTS. An earlier confirmatory shot was fired at LANL in December 2001. On those shots, P-22 fielded three diagnostics. A series of optical pins were used to record the arrival time of the expanding metal surface at preset distances. Free-surface optical pyrometry was used to measure the surface temperature of the plutonium at shock breakout. Four Asay windows (a VISAR diagnostic viewing the plutonium surface through a lithium-fluoride window) were used to diagnose the spall behavior of the plutonium.

The Armando SCE and its confirmatory shot are scheduled for April 2004. Both will be fired in the U1a complex. P-22 has played a significant role in the development and fielding of the Cygnus flash x-ray machines, which will be the primary diagnostic for the Armando shot. P-22 will also field free-surface optical pyrometry as a secondary diagnostic.

The Krakatau and Unicorn SCEs and their confirmatory shots are scheduled for FY 2005. Krakatau will be fired in the U1a complex, and Unicorn will be fired in a hole at U6c (which is in the Yucca Flats area of the NTS). The current plan for Krakatau calls for P-22 to field optical pins, free-surface pyrometry, multipoint VISAR, and possibly Asay windows. On Unicorn, P-22 will field a *reaction-history-like* gamma-ray-flux diagnostic, using field-test neutron generators to interrogate the package.

SNM Midcourse Detection

G.H. Nickel (P-22), R.E. Mischke, D.M. Lee (P-25)

In April 2003, LANL was asked by the Missile Defense Agency (MDA) to examine the feasibility of using the nuclear characteristics of special nuclear material (SNM) as a discrimination signature for a missile attack. The threat was presumed to consist of a single launch with many decoys—unlike the previous Strategic Defense Initiative work that considered hundreds of launch vehicles.

While the goal of this study was to determine the possible signature signals—not to develop an engineering design, the practicality of any proposed solution was important. Our team made comparisons to previous studies, actual deployed space systems, existing detectors, and reasonable extensions of current radiation-source technology. After considering a variety of sensors, our team determined that natural radiation or emissions created by cosmic rays would not be practical, except at distances of a few meters. The use of nondirectional active methods, such as neutron sources, would require extremely short ranges as well. Our team concluded that a highly directional active system such as an advanced neutral-particle accelerator, together with an array of detectors, could be feasible.

Our study was prepared and presented to the MDA "Blue Team" by members of P-DO, P-22, and P-24. The engineering design of such a system, although difficult, could be the subject of another study.

Sputtering from Fission Fragments

A. Klein, G.L. Morgan (P-23), D.G. Madland (T-16)

We are currently designing and constructing an experiment to measure the yield of neutral particles and clusters of particles that are sputtered from californium, uranium, and plutonium by internal fission. Although low-energy, heavy-ion-induced sputtering has been extensively studied for charged secondary ions, the neutral yield has so far only attracted scant interest because of the experimental difficulties of detecting neutral particles. In addition, conventional theoretical models, like the binary collision model (BCM) and molecular-dynamics (MD) calculations, will either breakdown at fission-fragment energies (BCM) or are currently impossible because of limited computer resources (MD).

Our setup will consist of an open source; a catcher foil, which will collect the sputtered material; and a silicon photodiode. All of the elements under study are decaying by alpha (α) decay. The silicon photodiode will measure the α activity of the sputtered material on the foil, thus allowing us to precisely determine the amount of material that has been desorbed from the target material. In a later stage of the experiment, we plan to measure the cluster size and energy distribution of the neutrals as well.

Laser-Driven Flyer Plates Generate Shock Waves in Weapons Materials

D.L. Paisley, D.C. Swift, T.E. Tierney, S. Luo, R.P. Johnson, C. Munson (P-24)

Laser-driven flyer plates can be used to impart shock waves into condensed-matter targets to study the results of dynamic shock-loading and release, similar to what happens in weapons systems. These plates can also be used in basic research to study the dynamics of materials (Figure 3). Using a laser to launch a one-dimensional flyer plate instead of using it to directly shock a material decouples the laser parameters from the flyer plate as it impacts a target material. A properly launched flyer plate resembles the projectile of a gas gun used to impact a target material, but it is usually smaller in size (8-mm in diameter). The smaller size of the laser-launched flyer plate without the normal sabot used in gas guns makes target recovery after an experiment much easier, especially with SNM, and mitigates most of the collateral damage to the target material. Laser-launched flyer plates can complement more traditional experimental methods and be used to perform unique experiments that may be difficult to do by other methods. The Trident laser at LANL can be configured with a long pulse length [2-μs full-width at half maximum (FWHM)] and greater than 500 J.

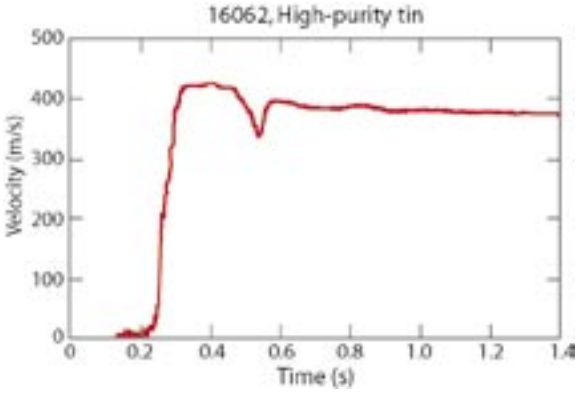

Figure 3. A laser-launched aluminum flyer plate is launched into a tin target, and the free surface of the tin is recorded by VISAR. The free-surface velocity profile obtained with VISAR allows us to determine the dynamic spall strength of the tin.

A 100–500 J, 2-μs FWHM temporal profile with a uniform spatial-profile laser beam is transmitted through a transparent substrate to an ablative layer sandwiched between the substrate and the flyer plate. As the laser energy is deposited in the ablative layer, the resulting "trapped" plasma expands and accelerates the flyer plate away from the substrate. Depending on aerial mass and energy, plate velocities of 0.1–5 km/s can be achieved. Currently, we are using 0.5- to1.5-mm thick flyer plates accelerated to 0.1–0.5 km/s to study the constitutive properties of weapons-related materials, and, in particular, the dynamic tensile strength (spall) as it relates to material composition and morphology. Flyer plates are launched into targets, and data are collected using multi-point VISAR and line interferometry as the primary diagnostics to measure shock and/or free-surface velocities. We anticipate Trident experiments to contribute an understanding to age-related changes in SNM that might affect the nation's enduring stockpile.

In-Line Holography for Ejecta Particle Size Measurements

D.S. Sorenson, D.R. Dillon, I.H. Campbell, W.T. Buttler, S.K. Lamoreaux (P-23), D. Tupa (P-25), R.P. Johnson (P-24), R.W. Minich (Lawrence Livermore National Laboratory), J.L. Romero (University of California, Davis), T.W. Tunnell, R. Fredrickson (Bechtel Nevada)

Holography has been used at NTS in the Cimarron and Thoroughbred shots at the U1a complex and at the Pegasus facility at LANL to measure ejecta-particle-size distributions. Ejecta are metal particles (solid or liquid) that are emitted from a shock-loaded surface. These measurements, in turn, allow us to calculate how the ejecta particles are transported in a gas environment.

The shape of the particle-size distribution reveals information about the fragmentation process. We are working toward a better understanding of how the particle-size distribution depends on the material properties of the shocked metal and an understanding of the shock-wave conditions. One of our goals is to develop a fragmentation model that we can apply to a variety of metals and pressure conditions. To advance this model, we have planned a series of experiments at the two-stage gas gun at LANL to measure particle-size distributions for shock-loaded tin for a range of pressures well below and above melt. We plan to extend these measurements using the TA-55 plutonium gas gun and Joint Actinide Shock Physics Experimental Research facility at NTS. As a part of this effort, we have built a frequency-doubled Nd:YAG high-power (0.6 GW) laser capable of providing a 120-mJ, 200-ps-wide laser pulse. The laser can be fired externally in single-shot mode. In addition, we are making improvements to the analysis programs used to reconstruct the particles. We have completed evaluating the laser and are in the final stages of designing the two-stage holography ejecta experiments.

Equation of State of Beryllium

D.C. Swift, R.P. Johnson, G.A. Kyrala, D.L. Paisley, T.E. Tierney (P-24), A. Hauer (P-DO), D.J. Thoma, J.C. Cooley (MST-6), M.D. Knudson (Sandia National Laboratories)

We used the flyer and ICE capabilities of the Z machine at SNL to investigate the EOS of beryllium to ~ 200 GPa on the STP (standard temperature and pressure) isentrope and around the principal shock Hugoniot—the locus of thermodynamic states that can be reached from a given initial state by the passage of shocks of different strength. This work was performed in support of the beryllium capsule design effort for ICF; our ultimate goal is to measure the onset of shock melting and hence to help control the seeding of ablative Rayleigh-Taylor instabilities.

In the flyer experiments, we impacted copper flyers traveling between ~ 7.5 and 9 km/s into samples of beryllium ~ 500 μm thick. The samples were backed by lithium-fluoride windows. We obtained laser Doppler velocimetry records at the beryllium/lithium-fluoride interface. In each experiment, the target assembly covered only half of the area of the flyer. We measured (also by Doppler velocimetry) the acceleration history of the flyer to characterize its state at the moment of impact.

Though superficially the shots seem quite simple, we had to include several corrections to explain features in the velocity history: the presence of a residual aluminum liner on the back of the copper flyers (we also performed control experiments with aluminum samples), residual drive pressure at the moment of impact, and the impedance mismatch between the beryllium sample and the lithium-fluoride window. The velocity histories exhibited additional features that may indicate shock or release melting. The peak interface velocity observed in each experiment—a measure of the EOS—was in good agreement with simulations using the published EOS for beryllium. Hugoniot points deduced from each experiment also matched the published Hugoniot EOS to within their uncertainty. Elastic precursor waves were expected to run ahead of the lower-pressure shock waves, but the velocity records did not have adequate time resolution to distinguish the precursors and, hence, to measure their amplitude, which would have helped verify models of plasticity in the 10- to 100-ns regime.

The ICE shot used beryllium samples ~ 250 and 500 μm thick to study the evolution of smooth compression waves as they propagated through the beryllium. Again, we obtained velocity histories by laser Doppler velocimetry. Between zero (i.e., the aluminum liner only) and 250 μm, the compression wave remained smooth and its evolution could be explained using the published EOS. Between 250 and 500 μm, the compression wave in the experiment apparently developed into a shock. This behavior was not reproduced in simulations using the same EOS—although the thicker experiments were subjected to a similar pressure history. The most likely explanation at present is that there were gaps in the assembly of the thicker samples, which would have led to the formation of shock waves.

The experiments on beryllium have demonstrated that published EOS from the SESAME and Steinberg compendia seem to be valid up to 200 GPa from the STP isentrope to the principal Hugoniot. We have elucidated some of the effects which need to be accounted for when interpreting detailed material response from flyer-impact experiments at Z. There may be some evidence for shock melting under conditions relevant to the ICF capsule.

Quantitative Ejecta and Timing Diagnostic Studies

W.T. Buttler (P-23), I.H. Campbell, D.R. Dillon, N.S.P. King, G.L. Morgan, J.R. Payton, D.S. Sorenson, M.D. Wilke (P-23), R.T. Olson, D.T. Westley, D.M. Oro (P-22), C.L. Morris (P-25), W.V. Anderson, F.G. Abeyta, M.E. Byers, R.S. Hixson, P.A. Rigg, D.L. Shampine (DX-2)

At LANL, we are quantitatively investigating the *Dynasen* piezoelectric pins as a useful, inexpensive alternative to the cumbersome Asay foils that require expensive, complex interferometric systems. We are considering two different *Dynasen* technologies: PZT and lithium niobate ($LiNbO_3$). To support this investigation, we have performed three series of gas-gun experiments in collaboration with DX-2 and P-22 to verify the static pin calibrations in regimes where material are known to be ejected from the vacuum-surface interface (ejecta). In the first series of experiments, configurations were such that the pressure profile was one-dimensional in nature. In addition, our experiments were performed with a supported shock, or a square pressure profile. The function of the grooves was to generate enough ejecta to be observed and characterized by an x-ray diagnostic fielded on each set of shots. In addition, most of the experiments included an Asay foil. The motivation of the different diagnostics was to independently compare areal densities as observed between the different technologies. Another set of experiments was performed on a different gas gun, using polished tin targets, a supported shock profile, x-ray diagnostics, piezoelectric pins, and Asay foils. A final set of experiments was performed with high explosives (unsupported shock, or *Taylor* wave) at NTS.

The probes themselves are thought to respond to viscous forces, such that the recorded voltage signal, $V(t)$, varies as the time derivative of the force: $F(t) = A\rho(t)u^2(t)$, where $\rho(t)$ is the ejecta volume density, $u(t)$ is the ejecta velocity, and A is the *normal* area of the piezoelectric material. The dynamic force is recovered from the measured piezoelectric-probe voltage, $V(t)$, by dividing by the termination resistance and probe sensitivity S ($S = 400$ pC-N^{-1} for the PZT and $S = 24$ pC-N^{-1} for the $LiNbO_3$), and then integrating the resulting corrected signal from the jump-off time to the time of arrival of the hard, free surface at the stationary probe. The probe is positioned at a well-defined distance behind the target. This result is then divided by the probe area A and the velocity of the ejected material, $u(t)$, and integrated again to recover the areal density of the material as a function of time. This result is then directly compared with the Asay foil results to determine whether the static sensitivity is accurate or whether there is a fixed, dynamic sensitivity that will accurately recover a quantitative representation of the observed Asay foil result; it is generally accepted that the Asay foil is a quantitative measurement.

The general conclusion of these experiments is that both technologies work well in a regime where the total areal density is at or below ~ 10–15 mg-cm^{-2}. As an upper limit on an appropriate regime, some experiments performed at LLNL were in good agreement at ~ 20 mg/cm^{-2}. The advantage of piezoelectric probes as compared to Asay-foil technology or x-ray diagnostics is the passive nature of the diagnostic and its low profile. Because of its profile, many tens of probes can be positioned to observe areal densities in tight, complex geometries. Lastly, the velocities, determined from the arrival of the free surface at the locations of the piezoelectric probes, have agreed to within 1–2% of velocities measured by other diagnostics, such as interferometry technology and x-ray diagnostics.

Friction Studies at pRad

G.A. Kyrala (P-24), J.E. Hammerberg (X-7), C.E. Ragan, III (X-5), K. Rainey (DX-3), D.A. Clark, B.J. Hollander, O.F. Garcia, K.A. Esquibel (P-22), C. Morris, D. Tupa, F.E. Merrill (P-25)

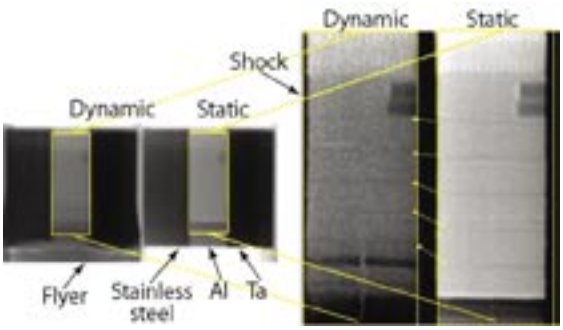

Figure 4. Diagram of the tantalum/aluminum/stainless-steel target with embedded tungsten wires.

This study is part of an LDRD-DR funded project, the "Physics Issues in Proton Radiography." This project's goal is to determine if pRad is a useful tool in friction studies. A secondary goal is to obtain data from a real target at slightly higher impact/shock velocities than those used on Atlas and Pegasus. Molecular-dynamic simulations show that the frictional force increases with sliding speed and then decreases to a very low value at the higher velocities. Frictional forces have been measured extensively at low velocities and low pressures (where the sliding speed is slower than the sound speed), but little has been done at higher velocities and higher pressures. The aim of our work is to establish the validity of the calculations in this intermediate regime using the imaging of implanted witness wires as a measure of the bending forces. Successful measurements using x-rays have been made on Pegasus but with limited spatial resolution. With the advent of well-developed tools for making measurements at the microscopic and mesoscopic scales, where a position resolution of < 15 μm over a 2-cm^2 field of view was demonstrated, we decided to take advantage of such a high-resolution tool for friction studies at the LANSCE pRad facility in Area C.

A friction experiment was fielded on October 16, 2003. This experiment used a flat-plate geometry, consisting of three 6-cm × 6-cm × 2-cm flat plates in the order (from right to left) of tantalum, aluminum (6061-T6), and stainless steel (21-6-9) (Figure 4). The target was impacted by a 15-mm-thick aluminum flyer plate at a nominal velocity of 2.2 mm/μs, driven by a Forrest flyer driver. In the midplane of the aluminum plate, a series of five 400-μm-diam wires were placed perpendicular to the tantalum/aluminum and stainless-steel/aluminum interfaces. The initial vertical wires are distorted near the interface during shock-loading as the aluminum shock outraces the tantalum and stainless-steel shocks. This loading results in a differential velocity along the interface, $0 < v < 1.1$ mm/μs, depending on the magnitude of the frictional force. Under these conditions, a steady state in pressure and relative velocity exists for a period of approximately 4 μs after shock arrival, after which release waves lead to significant unloading. During this time, the interface pressure is approximately $P = 200$ kbar with a relative velocity determined by the frictional force. Along with the radiographic measurement of wire configuration with time, a 7-point VISAR at the exit surface was employed to measure free-surface velocity at interfacial and noninterfacial sites as a check on the computational analysis and radiographic analysis of the wires. Initial results indicate a weaker frictional force than that measured in the Pegasus experiment, which was at slightly lower pressures and at one-half the flyer-impact velocity. This result (i.e., smaller or minimal bending at the pRad resolution) is consistent with a model that predicts a frictional force decreasing as a fractional power of the velocity [approximately as $v^{(-3/4)}$]. More extensive analysis of the data provided by this successful experiment is in progress.

Measurements of the Dynamic Properties of Beryllium Benefit the ICF and Weapons Program

D.C. Swift, D.L. Paisley, G.A. Kyrala, T.E. Tierney, S. Luo (P-24)

Scientists at SNL and LANL are supporting the weapons program and, at the same time, exploring new designs of fuel capsules for ICF by conducting experiments to study the EOS of beryllium and its properties (e.g., grain size, grain orientation, metal alloys, and solid-solid phase change). LANL's Trident laser and SNL's Z machine have allowed us to measure the EOS and flow stress in beryllium and to investigate solid-solid phase change and melt using flyer plates and ICEs. In collaboration with SNL, we have designed and conducted experiments on the Z machine using a multi-point VISAR as the primary

diagnostic. On Trident, we used VISAR, line interferometry, and transient x-ray diffraction as our primary diagnostics.

On Trident, we shocked 12- to 125-μm-thick beryllium foil samples and crystals by directly irradiating them with 30–200 J of laser energy for 1.0 and 2.5 ns, producing shock pressures up to 50 GPa (Figure 5). The primary feature that we were interested in was the elastic precursors that occurred at 0.7 km/s for the crystals and 0.5 km/s for the foils. On the Z machine, flyer plates were launched at beryllium targets to record shock on impact and/or particle velocity through the targets. Furthermore, we used the Z machine to study the effects of quasi-isentropic compression waves (at an estimated pressure of 195 GPa) in beryllium. These data will help define an ICF capsule design and provide weapon designers with additional information on beryllium. We will conduct further experiments on Trident, on the Z machine, and later at NIF to more fully understand how beryllium can be used in ICF capsules and provide data to weapons designers for code validation.

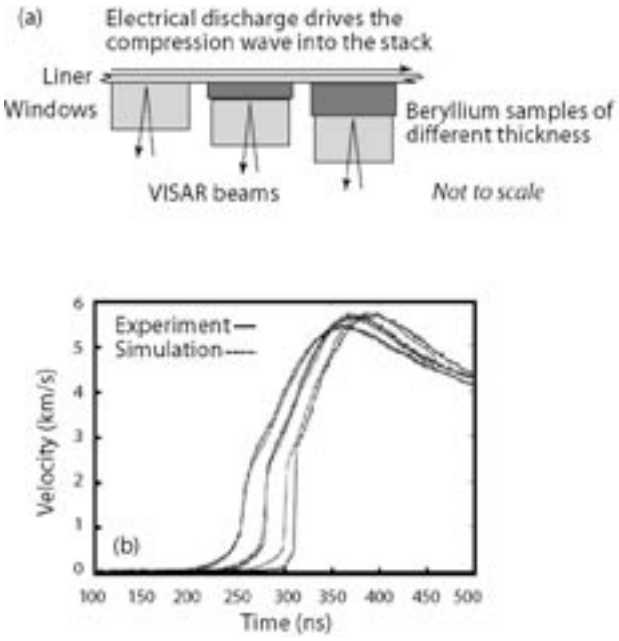

Figure 5. (a) A schematic of the quasi-ICE and (b) the comparison of an experimental result with simulation.

Development of well-validated material-failure-modeling capabilities requires both theoretical and experimental efforts. Because failure mechanisms depend strongly on material characteristics, it is difficult to predict the failure behavior of a material based on measurements made on other materials. Advances are needed to describe the complete physical processes and provide numerical-model implementation and testing. Model validation requires experiments that study phenomenology and material characterization, as well as more highly integrated validation experiments.

The pRad program at LANSCE delivers a multipulse capability that can produce a radiographic time sequence of dynamic systems. With the new capability to perform dynamic experiments that contain depleted uranium (DU), the pRad team was able to record a time sequence of the failure process in DU. We performed a series of experiments using 40-mm- and 80-mm-diam hemispherical shells of DU filled with high explosives. The explosive-loading accelerated a hemisphere into a biaxial stretching motion that led to material failure. We designed the experiments to study the failure process as a function of strain rate, initial shell thickness, and detonation configuration. The shot series included two 40-mm and two 80-mm DU hemispheres. A 40-mm steel hemisphere was also used to test new procedures and verify timing. All shots returned data that are currently being analyzed.

Figure 6 displays 4 of the 17 time-sequence transmission radiographs of the first 40-mm DU experiment. The evolution of the failure process towards a state where the material has fractured into cornflake-like pieces is clearly evident. Further analysis should yield estimates of DU density across the image, including fracture regions.

Failure-Mechanism Studies of Depleted Uranium Using Proton Radiography

K.B. Morley (P-23), for the Proton Radiography collaboration; L. Hull, P. Rightley, K. Prestridge (DX-3)

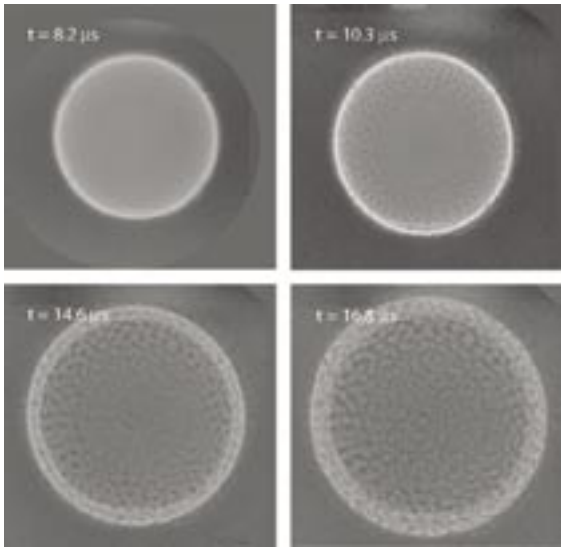

Figure 6. Transmission radiographs of the first 40-mm DU experiment; times are relative to the load ring.